ARTHROPOD SYSTEMATICS & PHYLOGENY

76 (3): 377–394
11.12.2018

SENCKENBERG

A comparative analysis of the ventral nerve cord of *Lithobius forficatus* (Lithobiomorpha): morphology, neuroanatomy, and individually identifiable neurons

Vanessa Schendel, Matthes Kenning & Andy Sombke*

University of Greifswald, Zoological Institute and Museum, Cytology and Evolutionary Biology, Soldmannstrasse 23, 17487 Greifswald, Germany; Vanessa Schendel [vanessa.schendel@web.de]; Matthes Kenning [matthes.kenning@googlemail.com]; Andy Sombke * [andy.sombke@gmx.de] — * Corresponding author

Accepted 19.iv.2018.
Published online at www.senckenberg.de/arthropod-systematics on 27.xi.2018.
Editors in charge: Markus Koch & Klaus-Dieter Klass

Abstract. In light of competing hypotheses on arthropod phylogeny, independent data are needed in addition to traditional morphology and modern molecular approaches. One promising approach involves comparisons of structure and development of the nervous system. In addition to arthropod brain and ventral nerve cord morphology and anatomy, individually identifiable neurons (IINs) provide new character sets for comparative neurophylogenetic analyses. However, very few species and transmitter systems have been investigated, and still fewer species of centipedes have been included in such analyses. In a multi-methodological approach, we analyze the ventral nerve cord of the centipede *Lithobius forficatus* using classical histology, X-ray micro-computed tomography and immunohistochemical experiments, combined with confocal laser-scanning microscopy to characterize walking leg ganglia and identify IINs using various neurotransmitters. In addition to the subesophageal ganglion, the ventral nerve cord of *L. forficatus* is composed of the forcipular ganglion, 15 well-separated walking leg ganglia, each associated with eight pairs of nerves, and the fused terminal ganglion. Within the medially fused hemiganglia, distinct neuropilar condensations are located in the ventral-most domain. Immunoreactive neurons of different transmitter systems (allatostatin, histamine, and FMRF-amide) display serially homologous patterns that may lay the foundation for comparison with other arthropod taxa. Moreover, a pair of histaminergic neurons may constitute a promising intra- as well as interspecific IIN candidate.

Key words. Arthropoda, centipedes, neuroanatomy, histology, immunohistochemistry, microCT, allatostatin, FMRF-amide, histamine.

1. Introduction

The central nervous system of arthropods is characterized by subdivision into brain and ventral nerve cord (Richter et al. 2010; Loesel et al. 2013), showing taxon-specific transformations and adaptations that are central to comparative neuroanatomical and phylogenetic studies (neurophylogeny *sensu* Harzsch 2006). In this context, myriapods play a crucial role, as their phylogenetic position still is a matter of debate. A widely accepted concept, which will be followed here, places the Myriapoda within the taxon Mandibulata as the sistergroup of a hexapod-crustacean clade (i.e. Tetraconata or Pancrustacea-hypothesis: Regier et al. 2010; Edgecombe 2010; Rota-Stabelli et al. 2011; Misof et al. 2014), as opposed to the Tracheata-hypothesis, proposing a myriapod-hexapod sistergroup relationship (e.g. Wägele & Kück 2014). Several morphological characters initially proposed to be apomorphic for Tetraconata were found to be present in representatives of Myriapoda as well, giving further support for the Mandibulata-hypothesis (Müller et al. 2003, 2007; Schachtner et al. 2005; Sombke et al. 2011a; Sombke et al. 2012; Sombke & Harzsch 2015).

Along these lines, neuromorphological and neuroanatomical characters proved to be a suitable character complex as they are considered rather robust over evolutionary time scales, and have been used in cladistic analyses resulting in well-resolved, yet still debated arthropod phylogenies (Strausfeld & Andrew 2011; Wolff et al. 2017). Detailed investigations on the ner-

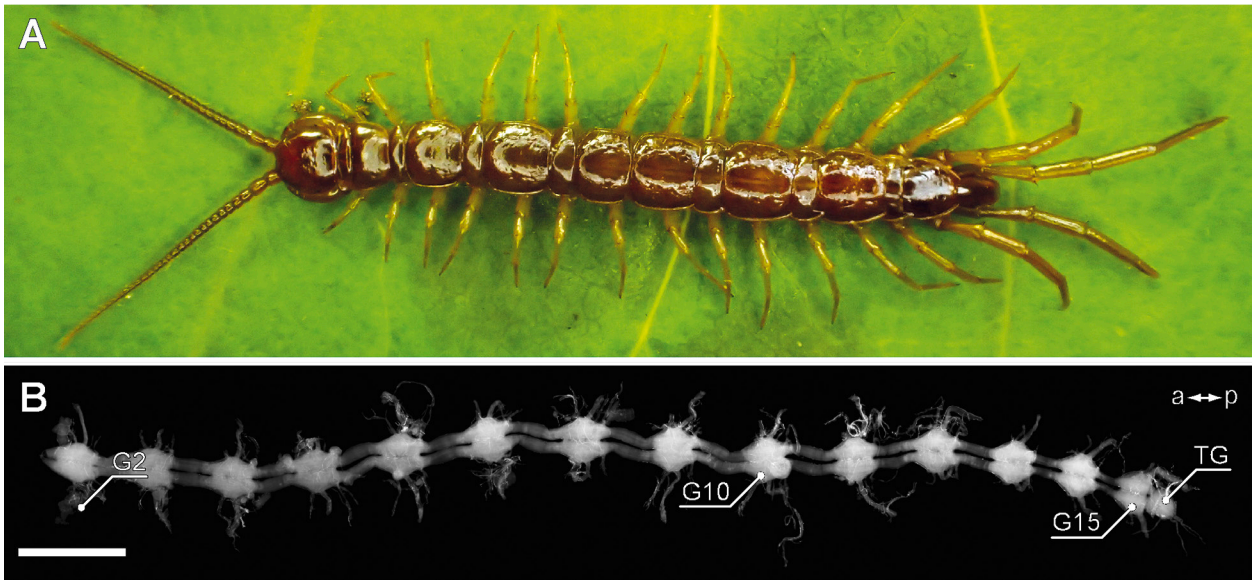

Fig. 1. *Lithobius forficatus* and dissected nervous system. **A**: Adult male of *Lithobius forficatus*, dorsal view. **B**: Dissected ventral nerve cord with walking leg ganglia 2 to 15 and terminal ganglion, dorsal view. The ganglia associated with the forcipular and first walking leg segments are omitted. — ***Scale bar***: 1 mm. — ***Abbreviations***: G: ganglion, TG: terminal ganglion.

vous system of Myriapoda, and specifically Chilopoda (centipedes), however, are few when compared to the wealth of studies conducted in Hexapoda and Crustacea (SOMBKE & ROSENBERG 2016). One promising field for comparative neuroanatomical analyses is the study of individually identifiable neurons (IINs) in the arthropod brain and ventral nerve cord (VNC). IINs can be identified and homologized intra- and interspecifically based on the specific criteria of position and morphology of somata and neurites, ontogenetic aspects, as well as physiological and biochemical characteristics (KUTSCH & BREIDBACH 1994). In particular, the neurotransmitter serotonin (5HT) has been studied comprehensively in a comparative context (THOMPSON et al. 1994; HARZSCH & WALOSZEK 2000; HARZSCH 2004; STEGNER et al. 2014; BRENNEIS & SCHOLTZ 2015; STEMME et al. 2017; SOMBKE & STEMME 2017). The first studies on lobsters, locusts and cockroaches pointed out striking morphological similarities of serotonergic neurons, inferring homologies at the single cell level (BELTZ & KRAVITZ 1983; BISHOP & O'SHEA 1983; TAGHERT & GOODMAN 1984). Thus easily assessable and low in neuron number, IINs constitute a suitable character complex in evolutionary discussions (KUTSCH & BREIDBACH 1994). Recent studies on centipedes revealed apomorphic characters for this taxon, but also synapomorphic characters with Tetraconata in soma positions and neurite trajectories, with implications for the reconstruction of the mandibulate ground pattern (SOMBKE & STEMME 2017). However, when considering the at least 50 known different neuropeptides and other classes of neuroactive substances present in arthropods (e.g. biogenic amines like histamine) (e.g. HOMBERG 1994; NÄSSEL 2000; GÄDE & MARCO 2006; CHRISTIE et al. 2011; CHRISTIE 2015), this serotonin-centric view leaves potentially informative characters unconsidered.

Five major lineages of Chilopoda are established. Scutigeromorpha are considered to be the most basal taxon and sistergroup to Pleurostigmophora. The latter comprises Lithobiomorpha and Phylactometria (Craterostigmomorpha and Epimorpha), with Epimorpha being composed of Scolopendromorpha and Geophilomorpha (EDGECOMBE 2011). Recently, this view has been challenged by transcriptomic data that place Lithobiomorpha as the sistergroup of Epimorpha, repositioning Craterostigmomorpha to a more basal node (FERNÁNDEZ et al. 2016). The centipede *Lithobius forficatus* (Linnaeus, 1758) is one of the best-studied myriapod species with respect to general anatomy and morphology and other biological fields, such as endocrinology, development, and physiology (MINELLI 2011). The trunk of *L. forficatus* is composed of the forcipular segment, 15 leg-bearing segments, three fused postpedal segments bearing a pair of gonopods, and a telson (MINELLI & KOCH 2011). The VNC is composed of 18 mostly well-separated ganglia: the subesophageal ganglion, the forcipular ganglion, 15 leg-associated ganglia, and the (fused) terminal ganglion. Each walking leg ganglion possesses eight pairs of nerves innervating e.g. the legs and trunk musculature (RILLING 1960, 1968; SOMBKE & STEMME 2017). Using histological techniques, morphology of the VNC was investigated sporadically from the early 19th century on (summarized in HILKEN et al. 2011; SOMBKE et al. 2011b), but apart from the contributions by HECKMANN & KUTSCH (1995) and SOMBKE & STEMME (2017), the internal neuroanatomy remains poorly known. Consequently, neuroanatomical data that include specific labeling of single neurons, or labeling against neuroactive substances in the brain and the VNC are sparse (HECKMANN & KUTSCH 1995; MELZER et al. 1996; PETYKÓ et al. 1996; HARZSCH 2004; SOMBKE et al. 2012; SOMBKE & STEMME 2017).

In order to gain deeper insights into centipede neuroanatomy, we investigate the VNC of *Lithobius forficatus*. In this multi-methodological approach, we use histology and X-ray micro-computed tomography, as well as histochemical and immunohistochemical experiments combined with confocal laser-scanning microscopy, to document external morphology and neuroanatomy of the walking leg ganglia. Also, we visualize individually identifiable neurons using a set of antibodies against two neuropeptide families (allatostatin, FMRF-amide) and the biogenic amine histamine. As comparable data that can be used to infer primary homology hypotheses are scarce, this contribution may provide a foundation for using additional neurotransmitter systems in order to explore arthropod individually identifiable neurons.

2. Material and methods

2.1. Experimental animals

Adult individuals of *Lithobius forficatus* (Linnaeus, 1758) (Fig. 1A) were collected under deadwood in Greifswald, Germany and kept in plastic boxes. They were provided with water once a week and small crickets (*Acheta domesticus*) every two weeks.

2.2. Paraffin histology

After anesthetization by cooling in a freezer, four adult specimens were fixed in Bouin's solution (Mulisch & Welsch 2015) overnight. Each specimen was cut into two parts (anterior and posterior) and preparations were washed in several changes of phosphate buffered saline (PBS: 0.1 M, pH 7.4), dehydrated in a graded ethanol series, incubated in a 1:1 solution of ethanol and tetrahydrofuran (Carl Roth, CP82.1) for 2 hours, pure tetrahydrofuran for 18 hours, and in a solution of 1:1 tetrahydrofuran and paraffin (Carl Roth, 6643.1) at 60°C for 24 hours. Finally, preparations were embedded in pure paraffin and sectioned (5 µm) with a motorized rotary microtome (Microm HM 360). Sections were stained with Azan according to Geidies (Schulze & Graupner 1960) and mounted in Roti-Histokitt II (Carl Roth, T160.1).

2.3. X-ray micro-computed tomography (microCT)

Two specimens were anesthetized in a freezer and fixed in Bouin's solution overnight. One animal was cut into three parts. The VNC was dissected from the second animal (Fig. 1B). The subsequent preparation followed the protocol by Sombke et al. (2015). Preparations were washed in several changes of PBS, dehydrated in a graded ethanol series (30 to 99%) and incubated in a 1% iodine solution (iodine resublimated in 99% ethanol; Carl Roth, X864.1) for 12 hours. Preparations were washed several times in pure ethanol and critical point dried using the automated dryer Leica EM CPD300 (Leica Microsystems). Finally, samples were fixed on insect pins with super glue. Scans were performed with a Zeiss Xradia MicroXCT-200 at 30 kV, 6 W and 1 second (10 × magnification) or 3 seconds (20 × magnification) exposure. Scan parameters were: (1) mid-trunk with 10 × objective lens unit resulting in 2.14 µm pixel size, (2) posterior-trunk with 10 × objective lens unit resulting in 1.99 µm pixel size, and (3) dissected nerve cord with 20 × objective lens unit resulting in 0.93 µm pixel size. Tomography projections were reconstructed using the XMReconstructor software (Zeiss Microscopy) resulting in image stacks (TIFF format). All scans were performed using binning 2 (resulting in noise reduction) and subsequently reconstructed using binning 1 (full resolution) to avoid information loss.

2.4. Immunohistochemistry and histochemistry

After anaesthetization, adult specimens were decapitated and pre-fixed in 4% paraformaldehyde (PFA) for 20 minutes. After removal of legs and tergites in PBS, samples were further fixed in PFA overnight at 4°C. For histamine-immunohistochemistry, specimens were pre-fixed overnight at 4°C in 4% N-(3-Dimethylaminopropyl)-N'-ethylcarbodiimide hydrochloride (EDAC; Sigma Aldrich, E6383) and then post-fixed in 4% PFA at room temperature for 4 hours. VNCs were dissected in PBS, washed in several changes of PBS-TX (0.5% Triton-X 100; Sigma Aldrich, X100) and incubated in blocking solution (0.5% Triton-X 100, 5% BSA [bovine serum albumin; Sigma, A2153]) for 4 hours. VNCs were incubated in primary antibodies: anti-A-type Dip-allatostatin 1 (Jena Bioscience, ABD-062; 1:2000), anti-FMRF-amide (ImmunoStar, 20091; 1:2000), and anti-histamine (Progen, 16043; 1:1000), for 96 hours at room temperature and washed in several changes of PBS-TX. Subsequently, preparations were incubated in secondary antibodies (anti-rabbit AlexaFluor-488 IgG; Invitrogen A11008, 1:500 and anti-mouse Cy3 IgG; Jackson ImmunoResearch 115-165-003, 1:500) or phalloidin (phalloidin Alexa-Fluor546; Molecular Probes, A22283; 1:50) for 48 hours at room temperature, and washed in several changes of PBS-TX (0.5% Triton-X 100) and finally in PBS. Preparations were mounted on adhesive microscope slides (HistoBond, Marienfeld) in glycerol. For additional experiments using anti-synapsin (anti-SYNORF1 concentrate, DSHB 3c11, 1:1000), specimens were treated according to Ott (2008). After dehydration, preparations were transferred to and scanned in methylsalycilate (Sigma Aldrich, W274518). In addition to whole-mount preparations, two VNCs were embedded in 4% agarose (Sigma Aldrich, A9414) and sectioned (100 µm) with a Zeiss Hyrax V50 vibratome. After permeabilization in

PBS-TX for 1 hour, sections were incubated in primary antibody (anti-A-type Dip-allatostatin) at 4°C for 18 hours, washed several times in PBS-TX and incubated in secondary antibody (see above) at 4°C for 18 hours. Preparations were washed in several changes of PBS and finally mounted on glass slides in Mowiol (Merck, 475904). Overall, data from 16 specimens using different labelings were used (anti-allatostatin n=4, anti-FMRF-amide n=3, anti-histamine n=5, anti-synapsin n=2, phalloidin n=2). All experiments were complemented by a nuclear counterstain using HOECHST (0.05%, bisBenzimid H 33258, Sigma Aldrich, 23491-45-4). However, the solution used produced a nonspecific broad band fluorescence resulting in a cross-talk between detector and nuclear counterstain.

Anti-A Dip-allatostatin 1 (rabbit, polyclonal) and anti-FMRF-amide (rabbit, polyclonal) as well as anti-synapsin (mouse, monoclonal) were previously used on the centipede *Scutigera coleoptrata* (Linnaeus, 1758). Peptide preadsorption and western blot experiments confirmed antibody specificity for that species (SOMBKE et al. 2011a). As we cannot exclude the possibility that the antibodies against allatostatin and FMRF-amide label a variety of peptides, we term labeled structures allatostatin-like and FMRF-amide-like immunoreactive (ASTir, RFir). Anti-histamine (rabbit, polyclonal) was also used on the centipede *S. coleoptrata* (SOMBKE & HARZSCH 2015). We will refer to the labeled structures in *L. forficatus* as histamine-like immunoreactive (HISir). We additionally tested specificity of the secondary antibody by replacing the primary antibody with PBS. These experiments resulted neither in specific, nor in unspecific labeling.

2.5. Microscopy, image processing and terminology

Paraffin sections were investigated and digitized with a Nikon Eclipse 90i microscope. Immunohistochemical and histochemical preparations were examined with a Leica SP5 II confocal microscope (cLSM). Projections of cLSM stacks were generated using Fiji (ImageJ v. 1.51f). Segmentation and volume rendering of microCT image stacks were performed using AMIRA 6.0.1 (FEI). Images were post-processed in Adobe Photoshop using global contrast and brightness adjustment features as well as black and white inversion. The neuroanatomical nomenclature follows RICHTER et al. (2010) and SOMBKE & ROSENBERG (2016). We refer to the ganglion of the first trunk segment (associated with the maxillipedes) as the forcipular ganglion, to ganglia of trunk segments 2–16 as the walking leg ganglia 1–15, and to the fused ganglion of the postpedal segments as the terminal ganglion.

In order to designate particular neurons as individually identifiable neurons (IIN), they had to fulfill the following criteria: they had to be present in the same location in (1) both hemiganglia, (2) in several different (but at least three) walking leg ganglia, and (3) in at least two different individuals. Moreover, neurite trajectories and specific neurotransmitters were considered in order to establish an IIN pattern for walking leg ganglia. The nonspecific broad band fluorescence of several somata (see above) was carefully evaluated in the scoring and designation of IINs. The authors are aware of possible implications regarding identifying particular neurons. However, the nuclear counterstain only labels the nucleus, and thus the signal is significantly smaller and fainter (yet the chromatin is still visible in some cases) as compared to a completely labeled neuron including its neurites.

In order to facilitate comparison of soma locations within a single ganglion, we specify localities according to the neuroaxis as anterior, central (indicated in the schematics as grey dashed abscissa), and posterior, as well as lateral and medial (indicated in the schematics as grey dashed ordinate), and combinations thereof.

2.6. Abbreviations

a – anterior; **ACM** – anterior centromedial neurons; **AL** – anterolateral neurons; **AM** – anteromedial neurons; **con** – connective; **d** – dorsal; **G** – ganglion; **hdg** – hindgut; **HG** – hemiganglion; **IIN** – individually indentifiable neuron; **M** – muscle; **N** – nerve; **nl** – neurilemma; **p** – posterior; **PCM** – posterior centromedial neurons; **PHAL** – phalloidin labeling; **PL** – posterolateral neurons; **PM1** – posteromedial neurons, anterior group; **PM2** – posteromedial neurons, posterior group; **S** – sternite; **SGp** – gonopodial sternite; **so** – soma; **SYN** – synapsin-immunoreactivity; **T** – tergite; **TG** – terminal ganglion; **TGp** – tergite of gonopodial segment; **v** – ventral; **vdf** – vas deferens; **VNC** – ventral nerve cord; **vnd** – ventral neuropilar domain.

3. Results

3.1. Morphology and neuroanatomy of walking leg ganglia

The ventral nerve cord consists of 18 discernible ganglia linked by paired connectives (Figs. 1B, 2B, 4A,D). Posterior to the subesophageal and forcipular ganglion, walking leg ganglia are of equal size and dimension (Fig. 1B). Eight nerves are associated with each walking leg hemiganglion (Figs. 2A,B, 5C; following the terminology by RILLING 1960): nerve N1, the proximally fused nerves N2 and N3, the proximally fused nerves N4 and N5, nerve N6, and the proximally fused nerves N7 and N8 (Figs. 2A,B, 5C). The joint root of N7 and N8 is located at the posterior-most margin of each ganglion (Figs. 2A,B, 4D, 5C). At least N4 and N5 innervate the walking leg. We found no indications for a median nerve (i.e. an unpaired longitudinal nerve between the connectives). The mus-

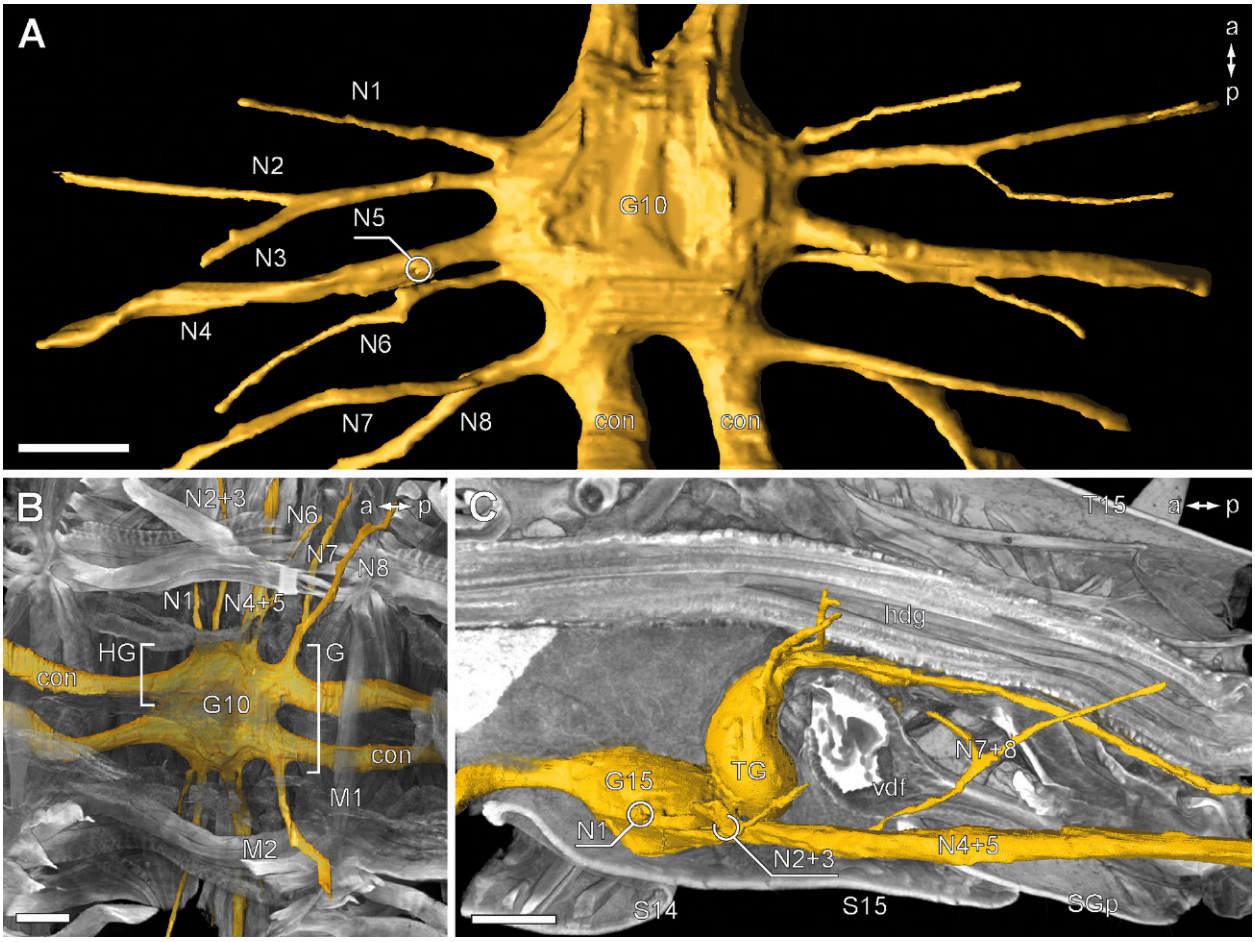

Fig. 2. MicroCT analysis of ventral nerve cord ganglia and nerve roots. External morphology. **A**: 3D reconstruction of walking leg ganglion G10, dorsal view. Eight pairs of nerves are associated with each hemiganglion. Nerves N2 and N3, N4 and N5, as well as N7 and N8 possess joint nerve roots. The small nerve N5 branches dorsally from nerve N4 (only proximal part reconstructed). Nerves N7 and N8 are located at the posteriormost border of the ganglion (compare Fig. 4D). **B**: The same ganglion (A) visualized within its anatomical context, dorsal view with virtual horizontal section of the trunk. Muscle M1 traverses the posterior connectives dorsally. Muscle M2 traverses all nerves except N8 dorsally. N8 projects further dorsally to innervate the dorsal heart nerve above the subsequent ganglion (not shown). **C**: Virtual sagittal section of the posterior trunk with reconstructed G15 (associated with the ultimate legs) and the fused terminal ganglion. Nerves N4 and N5 of G15 are directed posteriad (as appendages are directed posteriad). The neuraxis of the terminal ganglion is bent dorsad. Several nerves are associated with the terminal ganglion and innervate the caudal trunk. — ***Scale bars***: 200 µm. — ***Abbreviations***: con: connective, G: ganglion, hdg: hindgut, HG: hemiganglion, M: muscle, N: nerve, S: sternite, SGp: gonopodial sternite, T: tergite, vdf: vas deferens.

cle M1 traverses the posterior connectives dorsally (Figs. 2B, 4C,D). The smaller terminal ganglion (TG) succeeds the G15 without discernible connectives (Figs. 1B, 2C, 4A). However, a small central cavity between G15 and TG is visible after dissection (Fig. 1B). The neuraxis of the TG is prominently bent dorsad, which is not evident in dissected specimens (Figs. 1B vs. 2C, 4A). Several nerves are associated with the TG, innervating the caudal region (Fig. 2C). As the ultimate (or terminal) legs are held along the body axis, leg-associated nerves N4 and N5 of G15 project posteriad rather than laterad, as in the preceding walking leg ganglia (Fig. 2C).

MicroCT analysis reveals that the neurilemma surrounding the ganglion appears brighter due to a higher density than the nervous tissue of the ganglion (Fig. 3). Hemiganglia are medially fused; however, in the ganglion's midline there are several (up to seven) dorso-ventral penetrations sheathed by neurilemma (Fig. 3A,C,E; arrowheads). Several internal structures are discernible based on density differences. From the joint nerve root of N4 and N5, two major intraganglionic projections continue mediad (Fig. 3B,D; compare also anti-synapsin labeling in 5D). In cross sections, the dorsal projection could not be traced further. The ventral projection splits into a smaller, posteriad projecting portion and a larger, anteriad projecting portion (Fig. 3B,D; white semicircles) associated with the ventral neuropilar domain (Fig. 3B,D,F; vnd). Paraffin sections reveal that the neuronal somata form a cortex surrounding the ganglionic neuropil ventrally and laterally, while its dorsal surface and emanating connectives are mostly soma-free (Fig. 4). In contrast, the terminal ganglion is enveloped by a contiguous cortex (not shown). Similar to microCT analysis, paraffin histology indicates that dorso-ventral penetrations are sheathed by neurilemma (Fig. 4D; arrowheads). The ganglia are characterized by interweav-

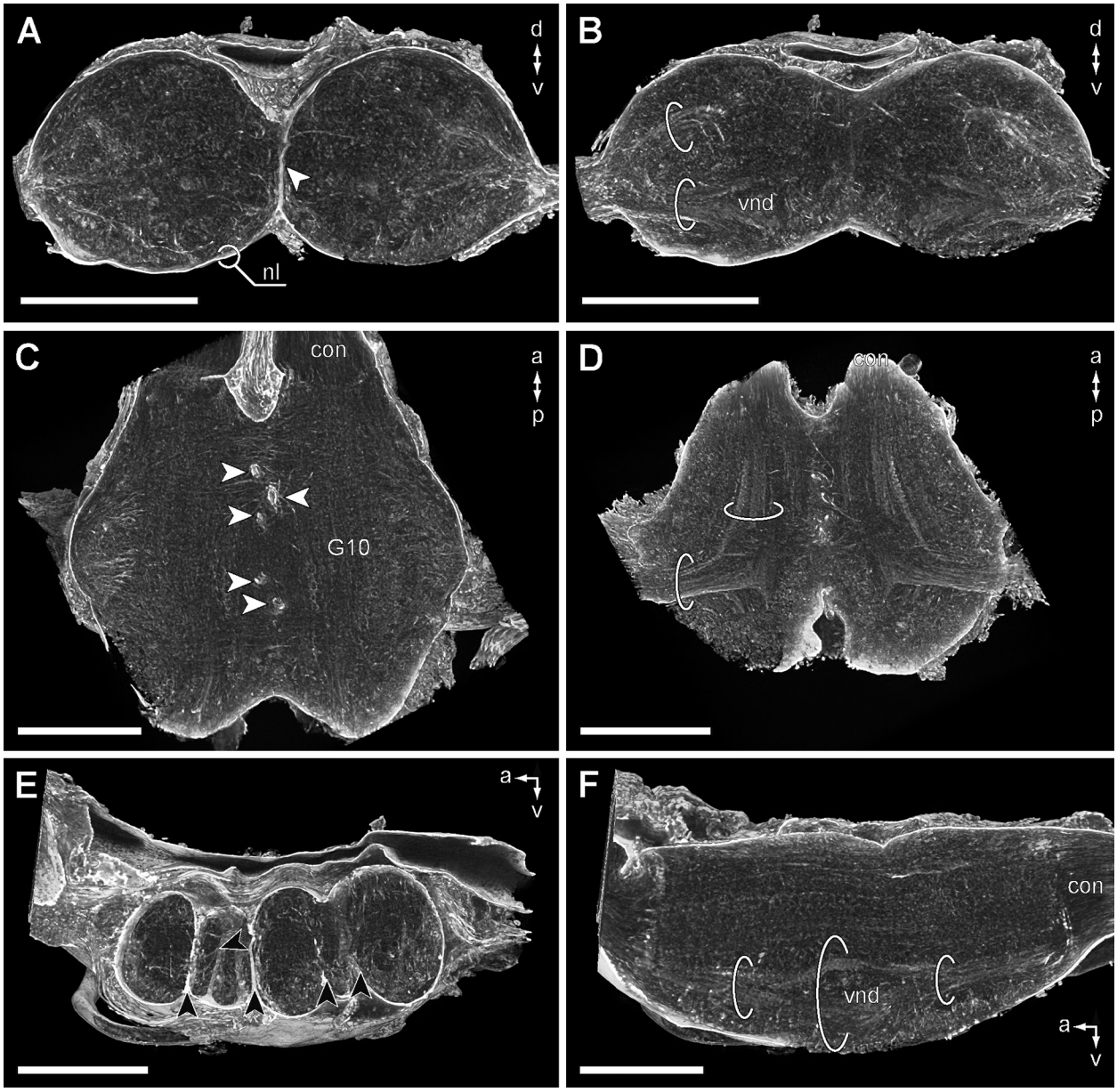

Fig. 3. MicroCT analysis of walking leg ganglion 10. Internal anatomy. **A**: Virtual cross-section. Note the brighter neurilemma and the median dorso-ventral penetrations sheathed by neurilemma (arrowhead). **B**: Virtual cross-section with intraganglionic projections from walking leg associated nerves N4 and N5. Projections target the dorsal and ventral areas of the hemiganglion. In the ventral part of the hemiganglion, a distinct ventral neuropilar domain (vnd) is evident. **C**: Virtual horizontal midsection. Dorso-ventral penetrations (arrowheads) penetrate the ganglion medially. Note the commissural neurites in the anterior part of the ganglion. **D**: Virtual horizontal section of the ventral domain. Neurites associated with nerves N4 and N5 project medially and further anteriorly and posteriorly. Longitudinal parallel elements of the ventral neuropilar domain are evident. **E**: Virtual sagittal midsection. Arrowheads mark dorso-ventral penetrations sheathed by neurilemma. **F**: Virtual sagittal section of a hemiganglion visualizing the ventral neuropilar domain with anteriad and posteriad projections. Note the parallel arrangement of neurites within the connectives. — ***Scale bars***: 100 µm. — ***Abbreviations***: con: connective, nl: neurilemma, vnd: ventral neuropilar domain.

ing neurites and dense neuropilar regions, while connectives are highly structured by parallel neurites (Fig. 4D). Paraffin histology likewise reveals a ventrally located neuropilar domain of slightly convoluted appearance with anteriad projection (Fig. 4B,D; compare Fig. 3D,F). Phalloidin labeling lends further insight into walking leg ganglion anatomy (Fig. 5A–C,E–G). The majority of neurites in the horizontal midsection proceed longitudinally (Fig. 5B), but no distinct tracts were identified. Several commissural neurites are found in the anterodorsal part of the ganglion (Fig. 5A, compare Fig. 3B,C); however, a distinct anterior or posterior commissure seems absent based on the applied methods. Sequential horizontal sections of a ganglion (Fig. 5E–G) highlight the structured ventral neuropilar domain, with two distinct innervations near the joint nerve root of N4 and N5 (Fig. 5D; white semicircle vs. black semicircles), anteriad and posteriad projections, and dense allantoidal (i.e. sausage-shaped) domains in its ventral-most area (Fig. 5G; arrows). Synapsin-immunoreactivity in whole

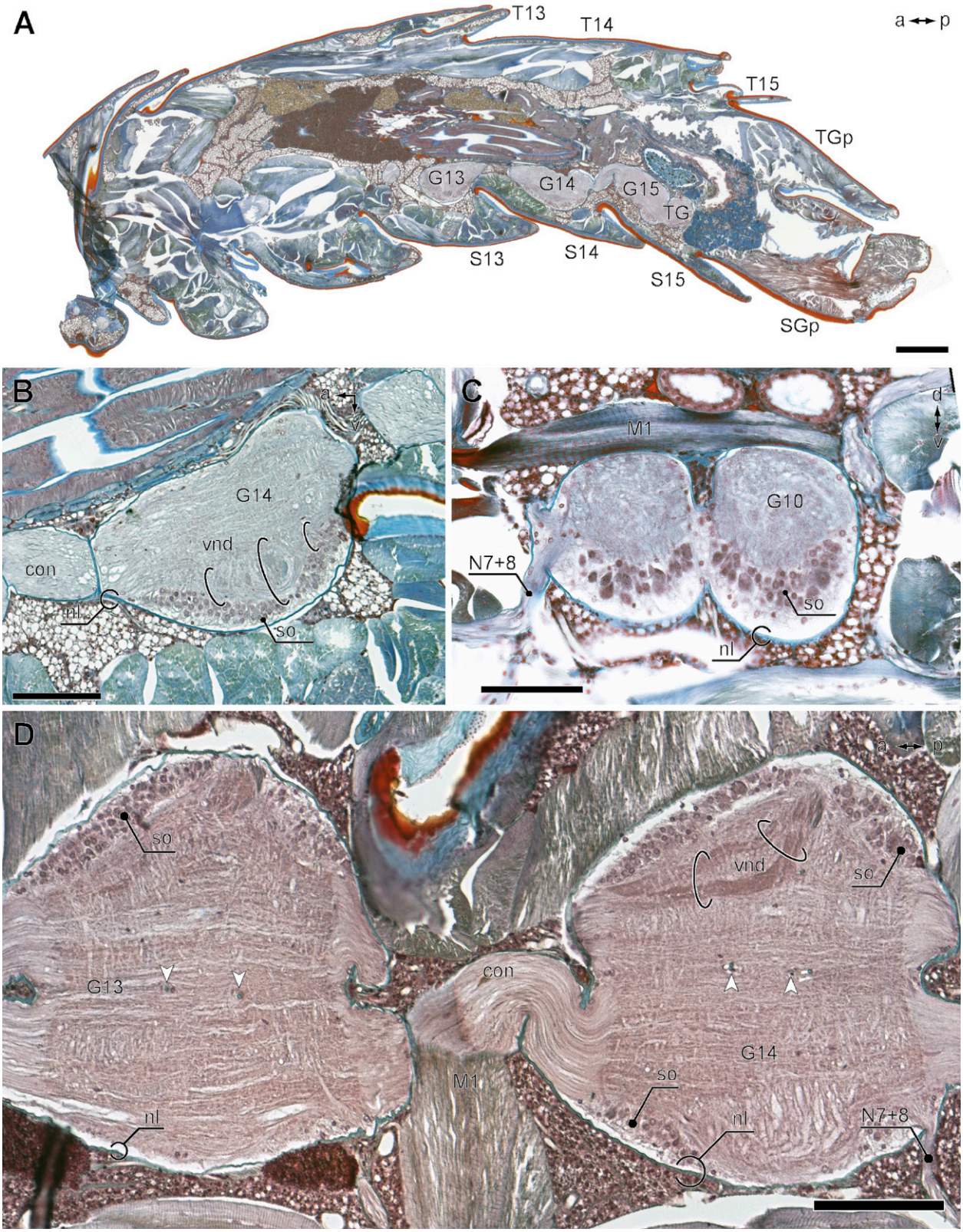

Fig. 4. Azan stained paraffin sections. **A**: Sagittal section of the posterior trunk with ganglia of the ventral nerve cord. Neuropilar domains are detectable in the ventral part of the ganglia (dark grey). Note the heteronomy of long and short tergites typical for Lithobiomorpha. **B**: Walking leg ganglion G14, sagittal section of a hemiganglion. The neurilemma (blue) coats the nervous system, somata are concentrated ventrally. Denser profiles of the ventral neuropilar domain are evident. **C**: Cross section of G10 (posterior region). Note that somata are concentrated ventrally. **D**: Horizontal section of G13 and G14, ventral area. In contrast to ganglia, connectives appear highly ordered by parallel neurites. Medially, ganglia are penetrated by dorso-ventral penetrations (arrowheads). Likewise, these penetrations are sheathed by a (blue) neurilemma. In G14 (right ganglion) projections from nerves N4 and N5 are evident. Ventral neuropilar domains are arranged in minor-convoluted elements with anteriad direction. Note the joint root of nerves N7 and N8. — ***Scale bars***: 200 µm. — ***Abbreviations***: con: connective, G: ganglion, M: muscle, N: nerve, nl: neurilemma, S: sternite, SGp: gonopodial sternite, so: soma, T: tergite, TG: terminal ganglion, TGp: tergite of gonopodial segment, vnd: ventral neuropilar domain.

mount preparations appears less structured, but indicates a similar pattern to phalloidin labeling (Fig. 5D). Within the ganglion, the joint nerve root of N4 and N5 splits into a dorsal and a ventral branch (compare Figs. 3B, 5E), which are associated with a thicker medial and thinner lateral domain, respectively. Both domains traverse the entire ganglion along its anteroposterior axis (Fig. 5D; compare Fig. 3D). In the connectives, there is no distinct anti-synapsin labeling.

3.2. Dip-allatostatin 1-like immunoreactivity (ASTir)

ASTir is distributed in the walking leg ganglia with several prominent longitudinal neurites, which are paramedially located in each hemiganglion (Fig. 6A; black semicircles). All labeled neurons are unipolar. Somata are located in anterior and posterior positions (Fig. 6B). In the anterior part of the ganglion, a pair of ASTir somata is located close to the midline (Fig. 6A,B; AM). Neurite trajectories could not be traced in detail, but might be ipsilateral, with further projections along the longitudinal ASTir neurites. In the posterior ganglion portion, two medially located groups of ASTir somata are present (Fig. 6A–C; PM1 and PM2). A slight variation in number (two or three) is detected in and between specimens. The more anterior group (PM1) consists of up to three somata; neurites project ipsilateral to the prominent longitudinal ASTir neurites (Fig. 6A–C). The more posterior group (PM2) consists of up to three ASTir somata (Fig. 6B,C). At least one neurite projects contralaterally (Fig. 6C). In few preparations, weakly labeled somata were detected in the posterolateral part of the ganglion (Fig. 6A; asterisks). In vibratome sections, but not in whole-mounts, two distinct commissural neurites (Fig. 6D) were detected in the dorsal-most region of walking leg ganglia. The two neurites traverse the entire ganglion at its posterior end, enclosing a dorsoventral penetration (Fig. 6D; black and white arrows). Their associated somata could not be identified.

3.3. FMRF-amide-like immunoreactivity (RFir)

RFir is distributed in the walking leg ganglia with several prominent longitudinal neurites in each hemiganglion (Fig. 7A; black semicircles). All labeled neurons are unipolar. Somata are located in anterior and posterior positions (Fig. 7B). Three RFir somata are located anterolaterally (Fig. 7A–C; AL). Neurite trajectories could not be traced further but probably remain ipsilateral, contributing to the longitudinal neurites. A cluster of RFir somata with contralateral projecting neurites is located anteromedially (Fig. 7A–F; AM). A single AM1 soma is located in the anterior-most part of the ganglion (Fig. 7C,E). Two AM2 somata are present slightly more posterior to AM1 (Fig. 7A–C,E). Their neurites project contralaterally in anterior direction, and further into the anterior connectives (Fig. 7A–D). In the preceding ganglion, these neurites enter the joint root of nerves N7 and N8 and project into both nerves (Fig. 7B,H). It remains unclear, however, which of the two neurons contributes to which nerve. A third group (AM3) is located paramedially between AM2 and AL (Fig. 7A–E). AM3 neurites project contralaterally and probably contribute to the longitudinal neurites (Fig. 7E,F). Another pair of RFir somata is located paramedially in the posterocentral part of the ganglion (Fig. 7A,B,G; PCM). Their neurites project medially, but it remains unclear whether they cross the midline or stay ipsilateral (Fig. 7G).

3.4. Histamine-like immunoreactivity (HISir)

HISir is sparsely distributed in the ganglia with thin longitudinal paramedial neurites in each hemiganglion (Fig. 8; black semicircles). All labeled neurons are unipolar. A centromedial cluster of three neurons is located slightly anterior to the center, possessing contralateral projecting neurites (Fig. 8A,B; ACM, black arrowheads). These neurites project to the lateral region of the ganglion close to the base of the nerve roots of N1–3. A single centromedial soma (PCM) with contralateral neurite projection is located slightly posterior to the center (Fig. 8A; black and white arrowheads). At the posterolateral border of the ganglion, the neurite of a single neuron (PL) projects anteromediad contributing to the ipsilateral longitudinal neurites (Fig. 8A,B; black arrows).

4. Discussion

4.1. External morphology of walking leg ganglia

The spectrum of methods applied shows that walking leg ganglia have comparable external morphology. Only in the ganglion associated with the ultimate legs (G15), nerves innervating the legs are directed posteriad. The results on external morphology are in concordance with most previous investigations and descriptions (VERHOEFF 1905; HANSTRÖM 1928; FAHLANDER 1938; RILLING 1960, 1968; HECKMANN & KUTSCH 1995; HARZSCH 2004; SOMBKE & STEMME 2017). The identity of trunk segments and walking leg ganglia may be confusing, as the first walking leg is associated with the third VNC ganglion, and the ultimate 15th legs are thus associated with the 17th VNC ganglion (SOMBKE & STEMME 2017). HARZSCH (2004) described 16 well-separated trunk ganglia (i.e. G1–G16, including the forcipular ganglion) and the terminal ganglion. We follow the description by RILLING (1960, 1968) counting the subesophageal ganglion, the

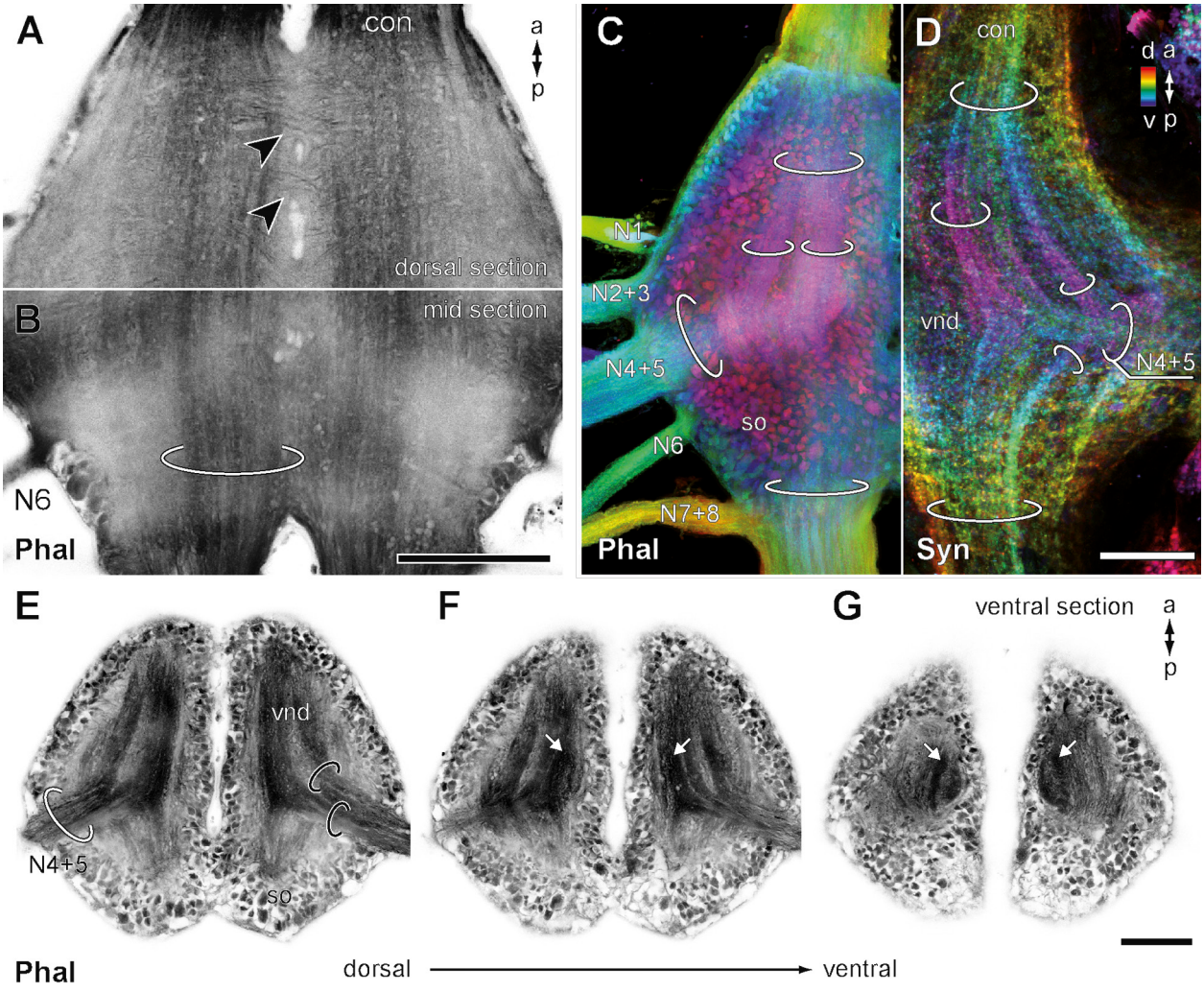

Fig. 5. Phalloidin histochemistry and synapsin-immunoreactivity (wholemounts). **A**: Phalloidin labeling in the anterodorsal G10; horizontal view showing commissural neurites (black arrowheads). White profiles are dorso-ventral penetrations. **B**: Phalloidin labeling in the posteromedial ganglion (G10); horizontal view. In contrast to (A), in the midsection the majority of neurites proceed longitudinally (white semicircle). **C**: Phalloidin labelling in G10; left hemiganglion, horizontal view, depth-color coded. Five nerve roots emerge from the ganglion. Based on color (depth) differences, actin richer areas are evident that corroborate microCT results (compare Fig. 3D) and synapsin-immunoreactivity (D). Projections associated with nerves N4 and N5 proceed mediad into the ganglion, condensing into distinct longitudinal tracts that traverse the hemiganglion in anteroposterior axis. **D**: Anti-synapsin labeling reveals several longitudinal domains that show a distinct immunoreactivity and traverse the entire ganglion in its anteroposterior axis. Both domains are associated with the nerves N4 and N5 (white semicircles, compare E), horizontal view. **E–G**: Virtual horizontal sections of a phalloidin labeled wholemount. The ventral neuropilar domain is associated with the joint nerve N4 and N5 (white semicircle) and innervated by two distinct branches (E; black semicircles) projecting anteriad as well as posteriad (E, F). **G**: Further ventrally and close to the peripheral cluster condensed allantoid domains are evident (white arrows). — ***Scale bars***: 100 µm. — ***Abbreviations***: con: connective, N: nerve, PHAL: phalloidin labeling, so: soma, SYN: synapsin-immunoreactivity, vnd: ventral neuropilar domain.

forcipular ganglion, 15 walking leg ganglia (G1–G15), and the fused terminal ganglion (TG). Rilling (1960) described that eight pairs of nerves are associated with each walking leg ganglion. This numbering was adopted by Heckmann & Kutsch (1995) and Harzsch (2004). Some nerves are fused proximally in a joint nerve root; different authors described a variable number: 5 (Fahlander 1938), 4 (Rilling 1968), or 6–8 (Heckmann & Kutsch 1995). In our samples, we found 5 separate nerve roots (N1, N2+N3, N4+N5, N6, N7+N8; Figs. 2A, 5C, 9). We did not detect a joint root of N1–3 as described by Rilling (1960, 1968) and Heckmann & Kutsch (1995). We found no indications of a median nerve (an unpaired nerve between the connectives), which was also not detected by Rilling (1960, 1968). Most of the eight nerves innervate trunk and walking leg musculature (Rilling 1960, 1968; Heckmann & Kutsch 1995). Nerves N1, N2 and N8 are described to be purely motoric, while the other five nerves (N3–N7) also contain sensory axons (Rilling 1968). According to Heckmann & Kutsch (1995), nerves N7 and N8 project into the posterior adjacent segment, targeting the dorsal longitudinal muscles (DLM) as well as the dorsal heart nerve, and the intersegmental muscle (ISM), respectively, which is in accordance with descriptions by Rilling (1960). This innervation pattern in *L. forficatus* is similar to the description in *Geophilus flavus*

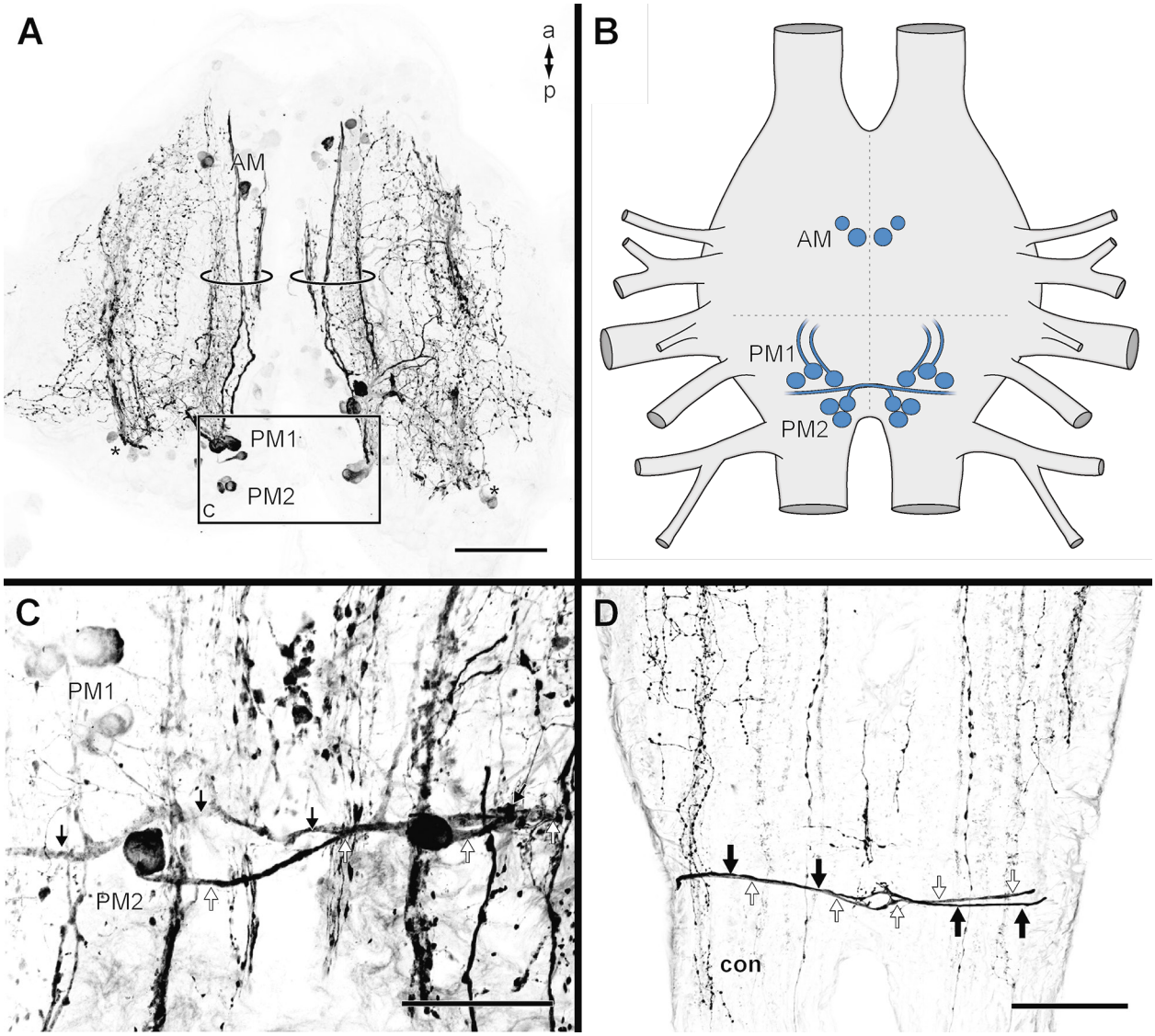

Fig. 6. Allatostatin-like immunoreactivity (ASTir) in walking leg ganglia (wholemounts and sections). **A**: Maximal projection of a 100 µm vibratome section showing anteromedial (AM) and posteromedial (PM1, PM2) cell clusters as well as longitudinal neurites (black semicircles). The asterisks indicate weakly labeled somata in the posterolateral part of the ganglion that were inconsistently found in few preparations, horizontal view. Box outlines details shown in C. **B**: Schematic representation of intraspecific individually identifiable ASTir neurons with identified neurite projection patterns. Grey dashed lines indicate ordinate as longitudinal midline and abscissa set at the joint root of N4+N5. **C**: Projection of a 100 µm vibratome section showing neurites of PM2 somata projecting contralaterally (white and black arrows), horizontal view **D**: Projection of a horizontal 100 µm vibratome section showing distinct commissural neurites traversing the ganglion latitudinal (black and white arrows) and enclosing a dorso-ventral penetration in the dorsalmost region of the posterior ganglion. Associated somata could not be identified. — ***Scale bars***: 100 µm. — ***Abbreviations***: AM: anteromedial neurons, PM1: posteromedial neurons (anterior group), PM2: posteromedial neurons (posterior group with contralateral projecting neurons).

(De Geer, 1778), where the posterior-most nerve (nervus dorsalis or segmental heart nerve) also innervates the dorsal heart nerve above the posterior adjacent ganglion (ERNST 1971). Our results on RFir additionally indicate an efferent contribution of the posteriorly adjacent segment, according to neurite trajectories. Consequently, N7+N8 are to be interpreted as intersegmental nerves. The term intersegmental nerve is often used in developmental studies, in which a nerve is established early on between two adjacent neuromeres, and is thoroughly documented for different tetraconate taxa (e.g. WHITINGTON et al. 1993; WHITINGTON 1995; HARZSCH et al. 1997; UNGERER & SCHOLTZ 2008). In all species, intersegmental nerves extend dorsally and innervate the musculature (and if applicable the heart). However, developmental studies in centipedes did not detect intersegmental nerves (WHITINGTON et al. 1991).

The ganglia of the VNC are sheathed by a neurilemma (Figs. 3A, 4B–E), which in arthropods serves as a barrier between hemolymph and nervous system, and consists mainly of collagen fibers and glia cells (FÜLLER 1964). The small dorso-ventral penetrations in the midline of ganglia are covered by the neurilemma and probably enclose tracheae. RILLING (1968) mentioned them as three to four 'median fibrils' (*mediane Fibrillen*), piercing the ganglion vertically.

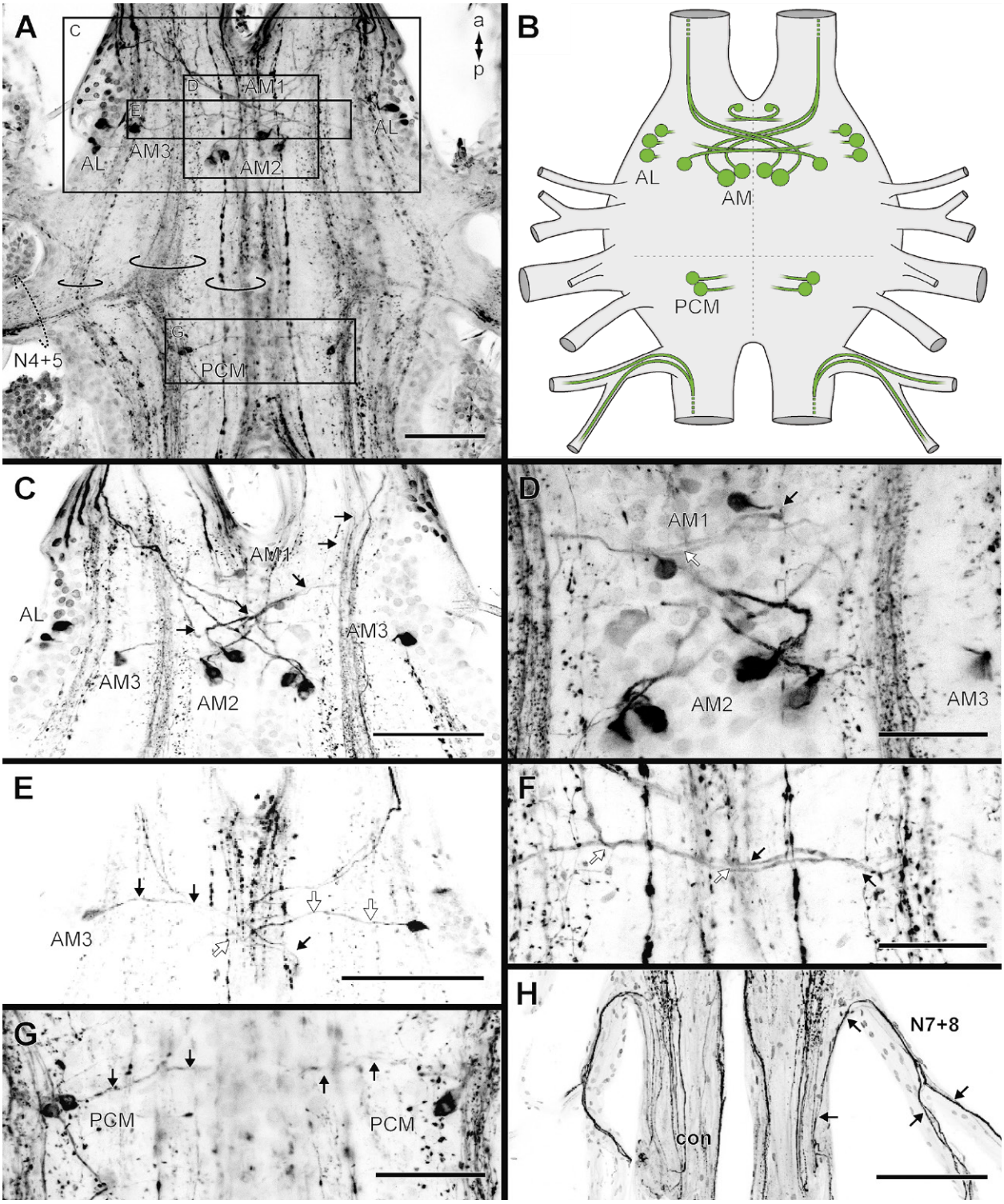

Fig. 7. FMRFamide-like immunoreactivity (RFir) in walking leg ganglia (wholemounts). **A**: Maximal projection of a ganglion with RFir neuron groups AL, AM1–3, PCM, and longitudinal neurites (black semicircles) in both hemiganglia, horizontal view. Dashed semicircles indicate the nerve root of N4 and N5. Boxes outline details shown in C,D,G,E. Grey dashed lines indicate ordinate as longitudinal midline and abscissa set at the joint root of N4+N5. **B**: Schematic representation of intraspecific individually identifiable RFir neurons with identified neurite projection patterns. **C**: Anterior part of the ganglion with anterolateral and anteromedial clusters 1–3. Black arrows indicate contralateral projecting neurites of AM2 neurons into the connectives. **D**: Anteromedial cluster of RFir somata (AM1–3). Neurites of AM1 neurons project contralaterally (black and white arrows). Neurites of AM2 neurons project contralaterally in anteriad direction and further into the anterior connectives. Neurites of AM3 neurons project contralaterally (compare E,F). **E**: AM3 neurons with contralaterally projecting neurites (black and white arrows). **F**: Contralaterally projecting neurites of AM3 neurons (black and white arrows). **G**: In the posterocentral part of the ganglion, a pair of RFir somata (PCM) is located paramedially with mediad neurite projection. **H**: Neurites from AM2 neurons enter the preceding ganglion and project into nerves N7 and N8 (black arrows, compare B,C). The faintly visible somata in A,C, and D are the result of a nonspecific broad band fluorescence of the nuclear counterstain. — ***Scale bars***: A,C,D,H 100 µm, E–G 50 µm. — ***Abbreviations***: AL: anterolateral neurons (with contralateral projections), AM: anteromedian neurons (with contralateral projections), con: connective, N: nerve, PCM: posterior centromedial neurons.

4.2. Anatomy of walking leg ganglia

As all walking legs are of comparable morphology, the neuroanatomy of ganglia G1–G14 likewise is similar. However, in *Lithobius forficatus* the last pair of legs is larger in size, and has a distinct morphology and non-locomotory function (KENNING et al. 2017). These differences are mirrored in the anatomy of G15, which will not be addressed here but comprehensively discussed in a separate contribution (KENNING et al. accepted). All ganglia of the VNC possess a peripheral cortex of variable thickness (with most somata located ventrally; Figs. 4, 5E–G) and a central neuropil that is most structured in the ventral area. Neuropilar regions could be consistently visualized by paraffin histology, microCT analysis, and phalloidin and anti-synapsin labeling. The most prominent neuropilar domains are associated with two branches, originating from the joint leg nerve N4 and N5 (compare Figs. 3B,D,F, 5C–G). These neuropils expand predominantly in the anterior direction. In phalloidin labeling, parallel arranged elements are detectable within the ventral neuropilar domain, which is corroborated by anti-synapsin-labeling. Moreover, in the ventral-most ganglion portion, distinct compact neuropilar domains are evident (Fig. 5E–G). In general, tetraconate VNC ganglia associated with appendages possess structured neuropilar domains. In hexapods, thoracic ganglia feature several dorsal longitudinal tracts of intersegmental neurites, a central neuropil of great complexity, and several ventral longitudinal tracts, as well as sensory neurites and associated neuropils in the ventral part of the ganglion (i.e. ventral association center VAC; BULLOCK & HORRIDGE 1965; PFLÜGER et al. 1981, 1988). Tetraconate VNC ganglia exhibit a strong structural correspondence, as this stereotypic organization is also found in crayfish (e.g. SKINNER 1985a,b; ELSON 1996). The VAC of locusts and crayfish as well as the ventral neuropilar domain in *L. forficatus* receive prominent afferent projections from leg-associated nerves. However, in locusts and crayfish, the neuropil appears either medially fused or strongly interconnected by commissural tracts, while in *L. forficatus* two distinct neuropilar regions without obvious contralateral connections are present (Figs. 3D, 5E–G). In order to further investigate efferent and afferent projections as well as interconnectivity of hemiganglia, additional experiments (e.g. selective backfilling) are desirable.

In many mandibulate taxa, at least one anterior and one posterior commissure connect both hemiganglia (LOESEL et al. 2013). In *L. forficatus*, hemiganglia are largely fused medially, and commissures within the ganglia are not evident. Although our experiments revealed commissural neurites, their condensation into prominent, densely packed midline spanning tracts appears only weakly pronounced (Fig. 5A, 6, 7, 9). In tetraconate arthropods, the anterior and posterior commissures have often been used as landmarks in describing specific structures within a ganglion, and when comparing somata positions of individually identifiable neurons in different taxa (e.g. HARZSCH & WALOSZEK 2000). However, BRENNEIS & SCHOLTZ (2015) – in their study of serotonergic neurons in Pycnogonida (Chelicerata) – noted that commissures may not always be a reliable criterion for comparing soma position, as not all representatives of Arthropoda possess a (single) anterior and posterior commissure. In *Lithobius forficatus*, ASTir, RFir, and HISir somata are located in the anterior and in the posterior parts of a ganglion. At least one neuronal pair (one neuron per hemiganglion) of each neurotransmitter investigated possesses contralaterally projecting neurites. Moreover, longitudinal neurites of respective transmitter systems are present in each hemiganglion. The only available data on single neurons in the VNC of *L. forficatus* (except for serotonergic neurons) were provided by HECKMANN & KUTSCH (1995) using $NiCl_2$ backfills, HARZSCH et al. (2005) using GABA immunohistochemistry, and AGRICOLA & BRÄUNIG (1995) demonstrating Perisulfakinin immunoreactivity. Perisulfakinin immunoreactive somata are located in most ganglia in a centrolateral position with neurite projections probably into nerve N6. GABAir revealed an anterior and a posterior cluster of inhibitory motoneurons as well as 2–5 neurons with contralateral projections. In comparison with tetraconate and chelicerate representatives, HARZSCH et al. (2005) concluded that inhibitory motoneurons, or groups thereof, in centipedes possess intriguingly similar characteristics in terms of soma location, anatomical features, and innervation patterns of leg muscles (HARZSCH et al. 2005; LOESEL et al. 2013). $NiCl_2$-backfills in walking leg ganglia (i.e. N7 of G3; Fig.10 in HECKMANN & KUTSCH 1995) revealed a highly arborizing termination domain in the respective hemiganglion. Additionally, ascending neurites pass through the posterior connectives and project into the posteriorly adjacent ganglion. The origin of respective neurites is a group of about 4 anteromedial somata in the contralateral hemisphere. This pattern of motoneurons innervating the ipsisegmental dorsal longitudinal muscles is rather similar to that seen in hexapods and crustaceans (see e.g. HECKMANN & KUTSCH 1995; WHITINGTON & BACON 1998). Although the identity of respective neurons remains unclear, this projection pattern is highly similar to that of the anteromedial RFir neurons in *L. forficatus*.

4.3. Individually identifiable neurons (IINs)

Based on the criteria of IINs by KUTSCH & BREIDBACH (1994), specific neurons can be identified intra- and interspecifically, and thus offer the possibility to establish homologies at the single cell level. Specific immunoreactive neurons in *Lithobius forficatus* were scored as IINs based on the criteria mentioned above (schematized in Figs. 6B, 7B, 8B, and 9). Regarding comparisons between different taxa, a wealth of studies described serotonergic neurons in various arthropods (HARZSCH & WALOSZEK 2000; HARZSCH 2004; BRENNEIS & SCHOLTZ 2015; STEMME et al. 2017; SOMBKE & STEMME 2017 and references therein), and in giving further support for

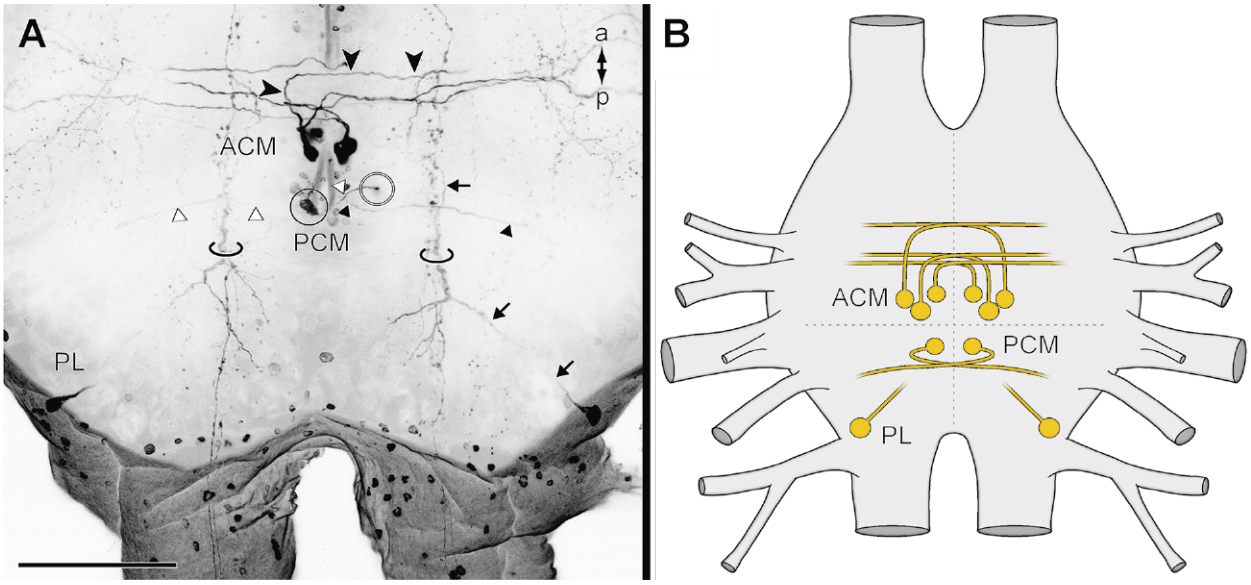

Fig. 8. Histamine-like immunoreactivity (HISir) in walking leg ganglia. **A**: Maximal projection of a wholemount, horizontal view. Within each hemiganglion, several HISir neuron clusters (ACM, PCM, PL) and characteristic thin longitudinal neurites (black semicircles) are visible. An anterior centromedial cluster (ACM) of three somata is located close to the midline possessing contralateral projecting neurites (black arrowheads). These neurites project into a diffuse HISir domain in the lateral region of the ganglion, close to the base of the nerve roots of N1 – 3. Further posterior, a single centromedial soma (PCM) with contralateral neurite projection is located (black and white arrowheads). At the posterolateral border of the ganglion, a single neuron (PL) with an anteromediad projecting neurite contributes to the longitudinal neurites (black arrows). **B**: Schematic representation of intraspecific individually identifiable HISir neurons with identified neurite projection patterns. The faintly visible somata in A are the result of a nonspecific broad band fluorescence of the nuclear counterstain. Grey dashed lines indicate ordinate as longitudinal midline and abscissa set at the joint root of N4+N5. — ***Scale bars***: 100 µm. — ***Abbreviations***: ACM: anterior centromedial neurons (with contralateral projections), PCM: posterior centromedial neurons, PL: posterolateral neurons.

Mandibulata, demonstrated the potential of IINs as independent characters in evolutionary considerations. In Mandibulata, serotonergic neurons are generally located in anterior, posterior, and central positions in VNC ganglia as recently discussed by Sombke & Stemme (2017). However, beyond the extensive research on arthropod serotonergic neurons, information on neurons in the arthropod VNC featuring other neurotransmitters is scarce, hampering further comparison and thus homologization.

The biogenic amine histamine is a common neurotransmitter in the visual system of arthropods (e.g. Battelle et al. 1991; Nässel 1999; Sombke & Harzsch 2015), and also present in the VNC. Within Hexapoda, a constant pattern is present with a single centro- to posteromedial pair of HISir somata in all ganglia, excluding the prothoracal ganglion of the VNC (Nässel et al. 1990; Nässel 1996; Hörner 1999). However, taxon-specific variations concerning number and size of additional somata and neurite trajectories occur. In investigated species, most neurites project ipsilateral with few contralateral branches in the anterior ganglion. In the cricket *Gryllus bimaculatus*, HISir neurites originating from various somata – including a ventromedial cluster – contribute to longitudinal HISir neurites (Hörner 1999). In *Calliphora vomitoria*, thinner longitudinal neurites traverse the ganglia both anteriorly and posteriorly, while thicker neurites project only anteriad. The respective somata are located in a ventromedial position (Nässel et al. 1990). Only few descriptions on HISir neurons for the crustacean and xiphosuran VNC are available (*Artemia salina*: Harzsch & Glötzner 2002; *Triops cancriformis*: Fritsch & Richter 2010; *Balanus nubilus*: Callaway & Stuart 1999; *Limulus polyphemus*: Harzsch et al. 2005). These descriptions mostly consider larval developmental aspects, and are thus of questionable comparability with the adult nervous system. Even so, late larval stages of *L. polyphemus* and *T. cancriformis* possess medial HISir somata. In contrast to representatives of Mandibulata, HISir somata are absent in the VNC of Arachnida. In the wandering spider *Cupiennius salei* and few other spiders, only three somata are located anteriorly to the arcuate body, with omnisegmental arborizations into all neuromeres of the synganglion and opisthosomal ganglion (Schmid & Duncker 1993; Schmid & Becherer 1999). In *Lithobius forficatus*, several centromedially situated HISir neurons, as well as lateral longitudinal neurites, are present. In comparison to representatives of Tetraconata, the number and position of somata (absence of anterolateral and presence of posterolateral neurons), and major projection patterns differ. However, our data, as well as published descriptions of histamine-immunoreactivity, indicate that the medial group of HISir neurons may be a promising candidate for the mandibulate ground pattern. Given that histamine-immunoreactivity can generally be compared with available antibodies, a much broader taxon sampling is both possible and desirable.

In contrast to serotonin and histamine, allatostatins and FMRF-amides are members of large peptide families (e.g. Orchard et al. 2001; Duve et al. 2002). Both antibodies used may label a variety of respective expressed

epitopes (A type allatostatins and FaRPs, respectively, see below); the criterion of a specific shared neurotransmitter in those putative IINs is rather problematic in terms of establishing interspecific comparability (SWALES & EVANS 1995). Apart from the focus on a neuroanatomical characterization of VNC ganglia in *L. forficatus*, the antibodies used revealed robust intraspecific patterns. This consequently raises the question of whether they can also be used in comparative investigations across arthropods. Allatostatins in general have been suggested to be conserved during invertebrate evolution, given their wide distribution (Cnidaria, Nematoda, Anellida, Mollusca, Arthropoda; SMART et al. 1994). In arthropods, they play a variety of physiological roles as regulatory neuropeptides (e.g. VITZTHUM et al. 1996). In the cockroach *Diploptera punctata*, seven allatostatins have been identified, and in the green shore crab *Carcinus maenas*, at least 20 members of the allatostatin familiy were isolated from thoracic ganglia (VITZTHUM et al. 1996; DUVE et al. 1997). ASTir neurons have been reported in the VNC of several species of Tetraconata (e.g. DUVE & THORPE 1994; VEELAERT et al. 1995; NÄSSEL 1996; MAESTRO et al. 1998; DIRCKSEN et al. 1999; DUVE et al. 2002). Dip-allatostatin 1 (APSGAQRLYGFGL-amide, the antibody applied in this contribution) has only been used in a few arthropod species to visualize neurons in the VNC (AGRICOLA & BRÄUNIG 1995; DIRCKSEN et al. 1999). In *Periplaneta americana*, a regular pattern of a single posterolateral ASTir neuron with anteriad projection is present in all abdominal ganglia. In abdominal ganglia 1–4, two additional medial somata are present (AGRICOLA & BRÄUNIG 1995). Within Crustacea, abdominal ganglia of *Orconectes limosus* house an undefined number of ASTir somata in anterolateral or lateral position, several somata of varying number in the ventral or ventromedial part, and several longitudinal ASTir neurites (DIRCKSEN et al. 1999). In contrast to tetraconate representatives, in VNC ganglia of *L. forficatus*, ASTir somata are located antero- and posteromedially. The tetrapeptide FMRF-amide and FMRF-amide-related peptides (FaRPs) are prevalent among various invertebrates and vertebrates (e.g. Hexapoda, NÄSSEL 1996; Nematoda, HENNE et al. 2017, PEYMEN 2014; Cnidaria, GRIMMELIKHUIJZEN & SPENCER 1984; Mollusca, MOROZ et al. 1994). For example, in *Periplaneta americana*, at least 23 peptides share the RFamide motif (PREDEL et al. 2004). RFir neurons have been reported in the VNC of crustacean and hexapod species, indicating a rather consistent distribution. In *Hutchinsoniella macracantha*, RFir neurons are present in the anterior part of the ganglion; in the crayfish *Procambaraus clarkii*, an anterolateral and a posterolateral cluster are present, along with several centromedial somata (MERCIER et al. 1991; ELOFSSON 1992). In *Schistocerca gregaria*, RFir neurons are present in anterolateral and centromedial and – depending on the antibody used – also in posterolateral position (FMRF-amide vs. SchistoFLRF-amide; SWALES & EVANS 1995; NÄSSEL 1996). In VNC ganglia of *L. forficatus*, RFir somata are located anterolaterally, anteromedially, and centromedially. As it remains to be determined which of the known allatostatins and FMRF-amide related peptides are expressed and recognized by both antibodies used, interspecific homologization in terms of the criteria of IINs (i.e. shared neurotransmitter) is impossible. The lack of data in further arthropod taxa currently hampers a broader comparison. Thus, for comparative interspecific analyses across arthropods, there is a need of specific antibodies, which recognize single peptides (without cross-reactions).

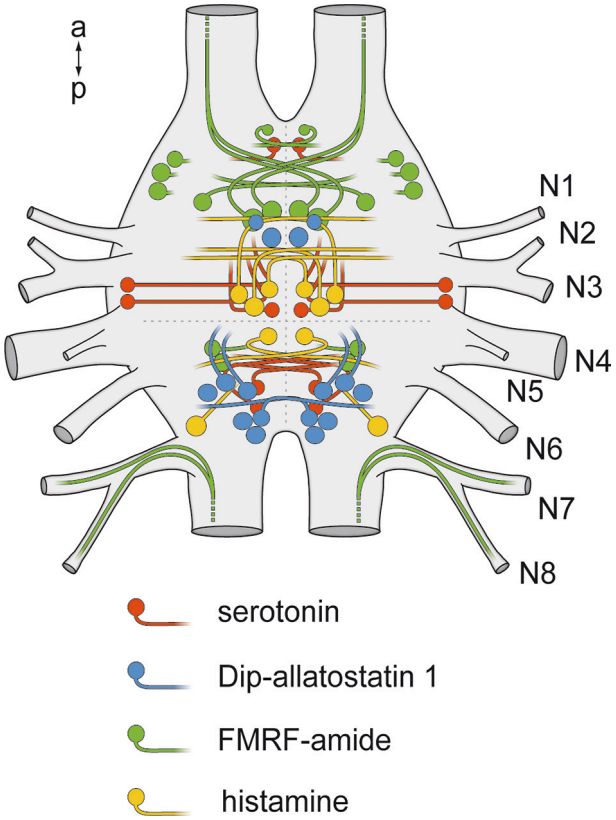

Fig. 9. Individually identifiable neurons of *Lithobius forficatus* walking leg ganglia. In addition to the neuropeptides analyzed in this contribution, serotonergic IINs as demonstrated in SOMBKE & STEMME (2017) are displayed. Grey dashed lines indicate ordinate as longitudinal midline and abscissa set at the joint root of N4+N5.

4.4. Neuronal characters for phylogenetic analyses

In terms of morphology-based phylogenetic reconstructions, using neuronal characters can be advantageous (at least on the level of higher ranking categories like orders), as the nervous system is not only evolutionarily stable, but also mostly independent of external morphological diversity (STRAUSFELD & ANDREW 2011). In Mandibulata, there are several examples of specific neuronal character sets (e.g. number, interconnectivity, and composition of subcompartments of deutocerebral chemosensory lobes and visual neuropils, or location and number of serotonergic neurons in the VNC) that can be used in support of phylogenetic relationships (e.g. SOMBKE et al. 2012; STRAUSFELD

2012; Sandeman et al. 2014; Sombke & Harzsch 2015; Schmidt 2016; Stemme et al. 2017; Sombke & Stemme 2017). Serotonergic neurons in the VNC were analyzed in numerous arthropod species and provide a character set for evolutionary considerations, as mentioned above. However, taxon sampling is often sparse, resulting in a lack of suitable data (especially with a focus on myriapods). Correspondingly, we provide the following list of morphological and anatomical characters (compiled from Heckmann & Kutsch 1995; Sombke et al. 2011b; Sombke & Rosenberg 2016; Stemme & Sombke 2017; this study) in the centipede *Lithobius forficatus* as a basis for comparative neuroanatomical research and subsequent cladistic analysis. Based on this approach, detailed analyses of additional centipede and millipede taxa are desirable to reconstruct neuronal ground patterns at specific taxonomic levels (e.g. Lithobiomorpha). Relying on evolutionary stability – and hence phylogenetic utility – of neuronal character sets, anatomical studies of diverse species of Scutigeromorpha and Craterostigmomorpha promise to contribute to the clarification of the ambiguous positioning of these taxa (e.g. Heterоterga-hypothesis *sensu* Ax 2000, or the position of Craterostigmomorpha *versus* Lithobiomorpha *sensu* Fernández et al. 2016).

Brain
- tripartite syncerebrum (protocerebrum, deutocerebrum, and tritocerebrum)

Protocerebrum
- protocerebral glands with paired nerve
- two visual neuropils (lamina and medulla)
- translaminar retinula cell axons
- kenyon cells, mushroom body pedunculus with contralaterally confluent connection

Deutocerebrum
- deutocerebral chemosensory lobe with typically 43 elongated olfactory glomeruli
- two olfactory glomeruli feature a contralateral connection
- corpus lamellosum (deutocerebral mechanosensory neuropil) composed of at least 4 neuropilar lamellae, with contralateral connection

Tritocerebrum
- frontal ganglion fused with tritocerebrum, with posteriad projecting nervus recurrens featuring a small hypocerebral ganglion

Ganglia of the ventral nerve cord
- rope-ladder-like VNC with 18 ganglia interconnected by paired connectives
- fused subesophageal ganglion formed by neuromeres of the mandibular, maxilla1, and maxilla2 segments
- segments of forcipule and 15 walking legs each with separate ganglia
- fused terminal ganglion
- all ganglia medially fused
- distinct commissures absent (but commissural neurites present)
- ganglia with continuous cortex (no distinct soma clusters), cortex thicker in the ventral part of the ganglia
- each walking leg hemiganglion associated with 8 nerves originating from 5 distinct nerve roots
- N7 and N8 are intersegmental nerves
- nerve N7 innervates the dorsal longitudinal muscles and the dorsal heart nerve (dorsally of posterior adjacent ganglion)
- nerve N8 innervates intersegmental muscle M10
- median nerve absent
- neuropilar condensations in the ventral ganglion (ventral neuropilar domain) with prominent anteriad and thinner posteriad projections

Individually identifiable neurons in walking leg hemiganglia
- 2 ASTir neurons in anteromedial position, unknown projections
- 3 ASTir neurons in posteromedial position, ispilateral projections
- 3 ASTir neurons in posteromedial position, contralateral projections
- 3 RFir neurons in anterolateral position, contralateral projections
- 4 RFir neurons in anteromedial position, contralateral projections (neurites of the two most medial neurons project into nerves N7 and N8 of the preceding anterior ganglion)
- 2 RFir neurons in posterior centromedial position, ipsilateral projections
- 3 HISir neurons in anterior centromedial position, contralateral projections
- 1 HISir neuron in posterior centromedial position, contralateral projection
- 1 HISir neuron in posterolateral position, ipsilateral projection
- 1 5HTir neuron in anteromedial position, ipsilateral projection
- 2 5HTir neurons in centrolateral position, ipsilateral projections
- 2 5HTir neurons in paramedial posterior position, contralateral projections
- 1 5HTir neuron in centromedial position, ipsilateral projection
- up to 13 motoneurons innervate the dorsolateral musculature (9 posteroventral and 4 anterodorsal somata, occasionally 2 additional centromedial somata)
- posteroventral motoneurons form dense dendritic fields
- anterodorsal motoneurons project into the preceding anterior ganglion
- the intersegmental muscle is innervated by six motoneurons located in the ventral ganglion

5. Acknowledgements

The authors thank Steffen Harzsch and Carsten H.G. Müller for technical support and discussions, and Monica Sheffer for helpful comments on the manuscript. We gratefully acknowledge the input provided by two anonymous reviewers that greatly improved the manuscript. This study was supported by DFG project SO 1289/1.

6. References

AGRICOLA H.-J., BRÄUNIG P. 1995. Comparative aspects of peptidergic signaling pathways in the nervous systems of arthropods. Pp. 303–327 in: BREIDBACH O., KUTSCH W. (eds), The Nervous Systems of Invertebrates: An Evolutionary and Comparative Approach. – Birkhäuser Verlag, Basel.

AX P. 2000. Multicellular Animals. The Phylogenetic System of the Metazoa. – Springer, Berlin Heidelberg.

BATTELLE B.-A., CALMAN B.G., ANDREWS A.W., GRIECO F.D., MLEZIVA M.B., CALLAWAY J.C., STUART A.E. 1991. Histamine: a putative afferent neurotransmitter in *Limulus* eyes. – Journal of Comparative Neurology **305**: 527–542.

BELTZ B.S., KRAVITZ E.A. 1983. Mapping of serotonin-like immunoreactivity in the lobster nervous system. – The Journal of Neuroscience **3**: 585–602.

BISHOP C.A., O'SHEA M. 1983. Serotonin immunreactive neurons in the central nervous system of an insect (*Periplaneta americana*). – Journal of Neurobiology **14**: 251–269.

BRENNEIS G., SCHOLTZ G. 2015. Serotonin-immunoreactivity in the ventral nerve cord of Pycnogonida – support for individually identifiable neurons as ancestral feature of the arthropod nervous system. – BMC Evolutionary Biology **15**: 136.

BULLOCK T.H., HORRIDGE G.A. 1965. Structure and Function in the Nervous Systems of Invertebrates. – W.H. Freemann and Company, San Francisco & London.

CALLAWAY J.C., STUART A.E. 1999. The distribution of histamine and serotonin in the barnacle's nervous system. – Microscopy Research and Technique **44**: 94–104.

CHRISTIE A.E. 2015. Neuropeptide discovery in *Symphylella vulgaris* (Myriapoda, Symphyla): *In silico* prediction of the first myriapod peptidome. – General and Comparative Endocrinology **223**: 73–86.

CHRISTIE A.E., NOLAN D.H., OHNO P., HARTLINE N., LENZ P.H. 2011. Identification of chelicerate neuropeptides using bioinformatics of publicly accessible expressed sequence tags. – General and Comparative Endocrinology **170**: 144–155.

DIRCKSEN H., SKIEBE P., ABEL B., AGRICOLA H., BUCHNER K., MUREN J.E., NÄSSEL D.R. 1999. Structure, distribution, and biological activity of novel members of the allatostatin family in the crayfish *Orconectes limosus*. – Peptides **20**: 695–712.

DUVE H., JOHNSEN A.H., SCOTT A.G., THORPE A. 2002. Allatostatins of the tiger prawn, *Penaeus monodon* (Crustacea: Penaeidea). – Peptides **23**: 1039–1051.

DUVE H., JOHNSEN A.H., MAESTRO J.-L., SCOTT, A.G., JAROS P.P., THORPE A. 1997. Isolation and identification of multiple neuropeptides of the allatostatin superfamily in the shore crab *Carcinus maenas*. – European Journal of Biochemistry **250**: 727–734.

DUVE H., THORPE A. 1994. Distribution and functional significance of Leu-callatostatins in the blowfly *Calliphora vomitoria*. – Cell and Tissue Research **276**: 367–379.

EDGECOMBE G.D. 2010. Arthropod phylogeny: An overview from the perspectives of morphology, molecular data and the fossil record. – Arthropod Structure & Development **39**: 74–87.

EDGECOMBE G.D. 2011. Chilopoda – Phylogeny. Pp. 339–354 in: A. MINELLI (ed.), Treatise on Zoology-Anatomy, Taxonomy, Biology. The Myriapoda. – Brill, Leiden.

ELOFSSON R. 1992. Monoaminergic and peptidergic neurons in the nervous system of *Hutchinsoniella macracantha* (Cephalocarida). – Journal of Crustacean Biology **12**: 531.

ELSON R.C. 1996. Neuroanatomy of a crayfish thoracic ganglion: Sensory and motor roots of the walking-leg nerves and possible homologies with insects. – The Journal of Comparative Neurology **365**: 1–17.

ERNST A. 1971. Licht- und elektronenmikroskopische Untersuchungen zur Neurosekretion bei *Geophilus longicornis* Leach unter besonderer Berücksichtigung der Neurohämalorgane. – Zeitschrift für Wissenschaftliche Zoologie (Leipzig) **182**: 62–130.

FAHLANDER K. 1938. Beiträge zur Anatomie und systematischen Einteilung der Chilopoden. – Zoologiska Bidrag fran Uppsala **17**: 1–148.

FERNÁNDEZ R., EDGECOMBE G.D., GIRIBET G. 2016. Exploring phylogenomic relationships within Myriapoda: should high matrix occupancy be the goal? – Systematic Biology **65**: 871–889.

FRITSCH M., RICHTER S. 2010. The formation of the nervous system during larval development in *Triops cancriformis* (Bosc) (Crustacea, Branchiopoda): An immunohistochemical survey. – Journal of Morphology **271**: 1457–1481.

FÜLLER H. 1964. Über Struktur und Chemismus der Neurallamelle bei Chilopoden. – Zeitschrift für Wissenschaftliche Zoologie (Leipzig) **169**: 203–215.

GÄDE G., MARCO H.G. 2006. Structure, function and mode of action of select arthropod neuropeptides. – Studies in Natural Products Chemistry **33**: 69–139.

GRIMMELIKHUIJZEN C.J.P., SPENCER A.N. 1984. FMRFamide Immunoreactivity in the nervous sytem of the medusa *Polyorchis penicillatus*. – The Journal of Comparative Neurology **230**: 361–371.

HANSTRÖM B. 1928. Vergleichende Anatomie des Nervensystems der Wirbellosen Tiere unter Berücksichtigung seiner Funktion. – Julius Springer Verlag, Berlin.

HARZSCH S. 2004. Phylogenetic comparison of serotonin-immunoreactive neurons in representatives of the Chilopoda, Diplopoda, and Chelicerata: implications for arthropod relationships. – Journal of Morphology **259**: 198–213.

HARZSCH S. 2006. Neurophylogeny: Architecture of the nervous system and a fresh view on arthropod phylogeny. – Integrative and Comparative Biology **46**: 162–194.

HARZSCH S., ANGER K., DAWIRS R.R. 1997. Immunocytochemical detection of acetylated alpha-tubulin and *Drosophila* synapsin in the embryonic crustacean nervous system. – International Journal of Developmental Biology **41**: 477–484.

HARZSCH S., GLÖTZNER J. 2002. An immunohistochemical study of structure and development of the nervous system in the brine shrimp *Artemia salina* Linnaeus, 1758 (Branchiopoda, Anostraca) with remarks on the evolution of the arthropod brain. – Arthropod Structure and Development **30**: 251–270.

HARZSCH S., WALOSZEK D. 2000. Serotonin-immunoreactive neurons in the ventral nerve cord of Crustacea: A character to study aspects of arthropod phylogeny. – Arthropod Structure and Development **29**: 307–322.

HARZSCH S., WILDT M., BATTELLE B., WALOSZEK D. 2005. Immunohistochemical localization of neurotransmitters in the nervous system of larval *Limulus polyphemus* (Chelicerata, Xiphosura): Evidence for a conserved protocerebral architecture in Euarthropoda. – Arthropod Structure and Development **34**: 327–342.

HARZSCH S., MÜLLER C.H.G., WOLF H. 2005. From variable to constant cell numbers: cellular characteristics of the arthropod nervous system argue against a sister-group relationship of Chelicerata and "Myriapoda" but favour the Mandibulata concept. – Development Genes and Evolution **215**: 53–68.

HECKMANN R., KUTSCH W. 1995. Motor supply of the dorsal longitudinal muscles II: Comparison of motoneurone sets in Tracheata. – Zoomorphology **115**: 197–211.

HENNE S., SOMBKE A., SCHMIDT-RHAESA A. 2017. Immunohistochemical analysis of the anterior nervous system of the free-living nematode *Plectus* spp. (Nematoda, Plectidae). – Zoomorphology **136**: 175–190.

HILKEN G., MINELLI A., MÜLLER C.H.G., ROSENBERG J., SOMBKE A., WIRKNER C.S. 2011. History of research. Pp. 20–42 in: A. MINELLI (ed.), Treatise on Zoology-Anatomy, Taxonomy, Biology. The Myriapoda. – Brill, Leiden, Boston.

HOMBERG U. 1994. Distribution of Neurotransmitters in the Insect Brain. – Gustav Fischer, Stuttgart, Jena, New York.

HÖRNER M. 1999. Cytoarchitecture of histamine-, dopamine-, serotonin- and octopamine-containing neurons in the cricket ventral nerve cord. – Microscopy Research and Technique **44**: 137–165.

Kenning M., Müller C.H.G., Sombke A. 2017. The ultimate legs of Chilopoda (Myriapoda): a review on their morphological disparity and functional variability. – PeerJ **5**:e4023.

Kenning M., Schendel V., Müller C.H.G., Sombke A. accepted. Comparative morphology of ultimate and walking legs in the centipede *Lithobius forficatus* (Myriapoda) with functional implications. – Zoological Letters.

Kutsch W., Breidbach O. 1994. Homologous structures in the nervous systems of Arthropoda. – Advances in Insect Physiology **24**: 1–113.

Loesel R., Wolf H., Kenning M., Harzsch S., Sombke A. 2013. Architectural principles and evolution of the arthropod central nervous system. Pp. 299–342 in: A. Minelli, G. Boxshall, G. Fusco (eds), Arthropod Biology and Evolution. – Springer Berlin Heidelberg, Berlin, Heidelberg.

Maestro J.L., Bellés X., Piulachs M.-D., Thorpe A., Duve H. 1998. Localization of allatostatin-immunoreactive material in the central nervous system, stomatogastric nervous system, and gut of the cockroach *Blattella germanica*. – Archives of Insect Biochemistry and Physiology **37**: 269–282.

Melzer R.R., Petykó Z., Smola U. 1996. Photoreceptor axons and optic neuropils in *Lithobius forficatus* (Linnaeus, 1758) (Chilopoda, Lithobiidae). – Zoologischer Anzeiger **235**: 177–182.

Mercier A.J., Orchard I., TeBrugge V. 1991. FMRFamide-like immunoreactivity in the crayfish nervous system. – Journal of Experimental Biology **156**: 519–538.

Minelli A. 2011. Treatise on Zoology-Anatomy, Taxonomy, Biology. The Myriapoda. – Brill, Leiden.

Minelli A., Koch M. 2011. Chilopoda - General Morphology. Pp. 43–66 in: A. Minelli (ed.), Treatise on Zoology-Anatomy, Taxonomy, Biology. The Myriapoda. – Brill, Leiden.

Misof B., Liu S., Meusemann K., Peters R.S., Donath A., Mayer C., Frandsen P.B., Ware J., Flouri T., Beutel R.G., Niehuis O., Petersen M., Izquierdo-Carrasco F., Wappler T., Rust J., Aberer A.J., Aspöck U., Aspöck H., Bartel D., Blanke A., Berger S., Böhm A., Buckley T.R., Calcott B., Chen J., Friedrich F., Fukui M., Fujita M., Greve C., Grobe P., Gu S., Huang Y., Jermiin L.S., Kawahara A.Y., Krogmann L., Kubiak M., Lanfear R., Letsch H., Li Y., Li Z., Li J., Lu H., Machida R., Mashimo Y., Kapli P., McKenna D.D., Meng G., Nakagaki Y., Navarrete-Heredia J.L., Ott M., Ou Y., Pass G., Podsiadlowski L., Pohl H., Reumont B.M. von, Schütte K., Sekiya K., Shimizu S., Slipinski A., Stamatakis A., Song W., Su X., Szucsich N.U., Tan M., Tan X., Tang M., Tang J., Timelthaler G., Tomizuka S., Trautwein M., Tong X., Uchifune T., Walzl M.G., Wiegmann B.M., Wilbrandt J., Wipfler B., Wong T.K.F., Wu Q., Wu G., Xie Y., Yang S., Yang Q., Yeates D.K., Yoshizawa K., Zhang Q., Zhang R., Zhang W., Zhang Y., Zhao J., Zhou C., Zhou L., Ziesmann T., Zou S., Li Y., Xu X., Zhang Y., Yang H., Wang J., Wang J., Kjer K.M., Zhou X. 2014. Phylogenomics resolves the timing and pattern of insect evolution. – Science **346**: 763–767.

Moroz L., Nezlin L., Elofsson R., Sakharov D. 1994. Serotonin- and FMRFamide-immunoreactive nerve elements in the chiton *Lepidopleurus asellus* (Mollusca, Polyplacophora). – Cell and Tissue Research **275**: 277–282.

Mulisch M., Welsch U. 2015. Romeis – Mikroskopische Technik. – Springer-Verlag.

Müller C.H.G., Rosenberg J., Richter S., Meyer-Rochow V.B. 2003. The compound eye of *Scutigera coleoptrata* (Linnaeus, 1758) (Chilopoda: Notostigmophora): an ultrastructural reinvestigation that adds support to the Mandibulata concept. – Zoomorphology **122**: 191–209.

Müller C.H.G., Sombke A., Rosenberg J. 2007. The fine structure of the eyes of some bristly millipedes (Penicillata, Diplopoda): Additional support for the homology of mandibulate ommatidia. – Arthropod Structure and Development **36**: 463–476.

Nässel D.R. 1996. Neuropeptides, amines and amino acids in an elementary insect ganglion: Functional and chemical anatomy of the unfused abdominal ganglion. – Progress in Neurobiology **48**: 325–420.

Nässel D.R. 1999. Histamine in the brain of insects: a review. – Microscopy Research and Technique **44**: 121–136.

Nässel D.R. 2000. Functional roles of neuropeptides in the insect central nervous system. – Naturwissenschaften **87**: 439–449.

Nässel D.R., Pirvola U., Panula P. 1990. Histaminelike immunoreactive neurons innervating putative neurohaemal areas and central neuropil in the thoraco-abdominal ganglia of the flies *Drosophila* and *Calliphora*. – The Journal of Comparative Neurology **297**: 525–536.

Orchard I., Lange A.B., Bendena W.G. 2001. FMRFamide-related peptides: a multifunctional family of structurally related neuropeptides in insects. – Advances in Insect Physiology **28**: 267–329.

Ott S.R. 2008. Confocal microscopy in large insect brains: Zinc-formaldehyde fixation improves synapsin immunostaining and preservation of morphology in whole-mounts. – Journal of Neuroscience Methods **172**: 220–230.

Petykó Z., Zimmermann T., Smola U., Melzer R.R. 1996. Central projections of Tömösváry's organ in *Lithobius forficatus* (Chilopoda, Lithobiidae). – Cell and Tissue Research **283**: 331 – 334.

Peymen K., Watteyne J., Frooninckx L., Schoofs L., Beets I. 2014. The FMRFamide-like peptide family in nematodes. – Frontiers in Endocrinology **5**: 90.

Pflüger H.J., Bräunig P., Hustert R. 1981. Distribution and specific central projections of mechanoreceptors in the thorax and proximal leg joints of locusts. – Cell and Tissue Research **216**: 79–96.

Pflüger H.-J., Braunig P., Hustert R. 1988. The organization of mechanosensory neuropiles in locust thoracic ganglia. – Philosophical Transactions of the Royal Society of London. Series B, Biological Sciences **321**: 1–26.

Predel R., Neupert S., Wicher D., Gundel M., Roth S., Derst C. 2004. Unique accumulation of neuropeptides in an insect: FMRFamide-related peptides in the cockroach, *Periplaneta americana*. – European Journal of Neuroscience **20**: 1499–1513.

Regier J.C., Shultz J.W., Zwick A., Hussey A., Ball B., Wetzer R., Martin J.W., Cunningham C.W. 2010. Arthropod relationships revealed by phylogenomic analysis of nuclear protein-coding sequences. – Nature **463**: 1079–1083.

Richter S., Loesel R., Purschke G., Schmidt-Rhaesa A., Scholtz G., Stach T., Vogt L., Wanninger A., Brenneis G., Doring C., Faller S., Fritsch M., Grobe P., Heuer C., Kaul S., Moller O., Muller C., Rieger V., Rothe B., Stegner M., Harzsch S. 2010. Invertebrate neurophylogeny: suggested terms and definitions for a neuroanatomical glossary. – Frontiers in Zoology **7**: 29.

Rilling G. 1960. Zur Anatomie des braunen Steinläufers *Lithobius forficatus* L. (Chilopoda). Skelettmuskelsystem, peripheres Nervensystem und Sinnesorgane des Rumpfes. – Zoologische Jahrbücher Abteilung für Anatomie und Ontogenie der Tiere **78**: 39–128.

Rilling G. 1968. *Lithobius forficatus*. Grosses Zoologisches Praktikum 13b. – Gustav Fischer Verlag, Stuttgart.

Rota-Stabelli O., Campbell L., Brinkmann H., Edgecombe G.D., Longhorn S.J., Peterson K.J., Pisani D., Philippe H., Telford M.J. 2011. A congruent solution to arthropod phylogeny: phylogenomics, microRNAs and morphology support monophyletic Mandibulata. – Proceedings of the Royal Society B: Biological Sciences **278**: 298–306.

Sandeman D.C., Kenning M., Harzsch S. 2014. Adaptive trends in malacostracan brain form and function related to behavior. Pp. 11–48 in: Derby C., Thiel M. (eds), Crustacean Nervous System and their control of behavior, The natural history of the Crustacea. – Oxford University Press, Oxford.

Schachtner J., Schmidt M., Homberg U. 2005. Organization and evolutionary trends of primary olfactory brain centers in Tetraconata (Crustacea & Hexapoda). – Arthropod Structure and Development **34**: 257–299.

Schmid A., Becherer C. 1999. Distribution of histamine in the CNS of different spiders. – Micrsoscopy Research and Technique **44**: 81–93.

SCHMID A., DUNCKER M. 1993. Histamine immunoreactivity in the central nervous system of the spider *Cupiennius salei*. – Cell and Tissue Research **273**: 533–545.

SCHMIDT M. 2016. Malacostraca. Pp. 529–582 in: SCHMIDT-RHAESA A., HARZSCH S., PURSCHKE G. (eds), Structure and Evolution of Invertebrate Nervous Systems. – Oxford University Press, Oxford.

SCHULZE E., GRAUPNER H. 1960. Anleitung zum mikroskopisch-technischen Arbeiten in Biologie und Medizin (GEEST and PORTIG, eds). – Akademische Vertragsgesellschaft, Leipzig.

SEIFERT G. 1967. Der Ursprung des dorsalen Herznervs der Lithobiiden (Chilopoda). – Experientia **23**: 452–453.

SKINNER K. 1985a. The structure of the fourth abdominal ganglion of the crayfish, *Procambarus clarki* (Girard). I. Tracts in the ganglionic core. – The Journal of Comparative Neurology **234**: 168–181.

SKINNER K. 1985b. The structure of the fourth abdominal ganglion of the crayfish, *Procambarus clarki* (girard). II. Synaptic neuropils. – The Journal of Comparative Neurology **234**: 182–191.

SMART D., JOHNSTON C.F., CURRY W.J., WILLIAMSON R., MAULE A.G., SKUCE P.J., SHAW C., HALTON D.W., BUCHANAN K.D. 1994. Peptides related to the *Diploptera punctata* allatostatins in nonarthropod invertebrates: An immunocytochemical survey. – The Journal of Comparative Neurology **347**: 426–432.

SOMBKE A., HARZSCH S. 2015. Immunolocalization of histamine in the optic neuropils of *Scutigera coleoptrata* (Myriapoda: Chilopoda) reveals the basal organization of visual systems in Mandibulata. – Neuroscience Letters **594**: 111–116.

SOMBKE A., HARZSCH S., HANSSON B.S. 2011a. Organization of deutocerebral neuropils and olfactory behavior in the centipede *Scutigera coleoptrata* (Linnaeus, 1758) (Myriapoda: Chilopoda). – Chemical Senses **36**: 43–61.

SOMBKE A., LIPKE E., KENNING M., MÜLLER C.H., HANSSON B.S., HARZSCH S. 2012. Comparative analysis of deutocerebral neuropils in Chilopoda (Myriapoda): implications for the evolution of the arthropod olfactory system and support for the Mandibulata concept. – BMC Neuroscience **13**: 1.

SOMBKE A., LIPKE E., MICHALIK P., UHL G., HARZSCH S. 2015. Potential and limitations of X-Ray micro-computed tomography in arthropod neuroanatomy: A methodological and comparative survey. – Journal of Comparative Neurology **523**: 1281–1295.

SOMBKE A., ROSENBERG J. 2016. Myriapoda. Pp. 478–491 in: SCHMIDT-RHAESA A., HARZSCH S., PURSCHKE G. (eds), Structure and Evolution of Invertebrate Nervous Systems. – Oxford University Press, Oxford.

SOMBKE A., ROSENBERG J., HILKEN G. 2011b. Chilopoda – The Nervous System. Pp. 217–234 in: MINELLI A. (ed.), Treatise on Zoology-Anatomy, Taxonomy, Biology. The Myriapoda. – Brill, Leiden.

SOMBKE A., STEMME T. 2017. Serotonergic neurons in the ventral nerve cord of Chilopoda - a mandibulate pattern of individually identifiable neurons. – Zoological Letters **3**: 9.

STEGNER M.E.J., BRENNEIS G., RICHTER S. 2014. The ventral nerve cord in Cephalocarida (Crustacea): New insights into the ground pattern of Tetraconata: Ventral Nerve Cord in Cephalocarida. – Journal of Morphology **275**: 269–294.

STEMME T., STERN M., BICKER G. 2017. Serotonin-containing neurons in basal insects: In search of ground patterns among tetraconata: Serotonin Neurons of Basal Insects. – Journal of Comparative Neurology **525**: 79–115.

STRAUSFELD N.J. 2012. Arthropod Brains. Evolution, functional elegance, and historical significance. – Belknap, Cambridge.

STRAUSFELD N.J., ANDREW D.R. 2011. A new view of insect-crustacean relationships I. Inferences from neural cladistics and comparative neuroanatomy. – Arthropod Structure & Development **40**: 276–288.

SWALES L.S., EVANS P.D. 1995. Distribution of SchistoFLRFamide-like immunoreactivity in the adult ventral nervous system of the locust, *Schistocerca gregaria*. – Cell and Tissue Research **281**: 339–348.

TAGHERT P.H., GOODMAN C.S. 1984. Cell determination and differentiation of identified serotonin-immunoreactive neurons in the grasshopper embryo. – The Journal of Neuroscience **4**: 989–1000.

THOMPSON K.S.J., ZEIDLER M.P., BACON J.P. 1994. Comparative anatomy of serotonin-like immunoreactive neurons in isopods: Putative homologues in several species. – The Journal of Comparative Neurology **347**: 553–569.

UNGERER P., SCHOLTZ G. 2008. Filling the gap between identified neuroblasts and neurons in crustaceans adds new support for Tetraconata. – Proceedings of the Royal Society of London B: Biological Sciences **1633**: 369–376.

VEELAERT D., SCHOOFS L., TOBE S.S., YU C.G., VULLINGS H.G.B., COUILLAUD F., LOOF A.D. 1995. Immunological evidence for an allatostatin-like neuropeptide in the central nervous system of *Schistocerca gregaria*, *Locusta migratoria* and *Neobellieria bullata*. – Cell and Tissue Research **279**: 601–611.

VERHOEFF K.W. 1905. Über die Entwicklungsstufen der Steinläufer, Lithobiiden, und Beiträge zur Kenntnis der Chilopoden. – Zoologische Jahrbücher: Zeitschrift für Systematik, Geographie und Biologie der Tiere; Unterreihe: Supplement **8**: 195–289.

VITZTHUM H., HOMBERG U., AGRICOLA H. 1996. Distribution of Dip-allatostatin I-like immunoreactivity in the brain of the locust *Schistocerca gregaria* with detailed analysis of immunostaining in the central complex. – The Journal of Comparative Neurology **369**: 419–437.

WÄGELE J.W., KÜCK P. 2014. Arthropod phylogeny and the origin of Tracheata (= Atelocerata) from Remipedia-like ancestors. Pp. 285–341 in: WÄGELE J.W., BARTOLOMAEUS T., MISOF B., VOGT L. (eds), Deep Metazoan Phylogeny: The Backbone of the Tree of Life. – De Gruyter, Berlin.

WHITINGTON P.M. 1995. Conservation versus change in early axonogenesis in arthropod embryos: A comparison between myriapods, crustaceans and insects. Pp. 181–219 in: BREIDBACH O., KUTSCH W. (eds), The Nervous System of Invertebrates: An Evolutionary and Comparative Approach. – Birkhäuser, Basel.

WHITINGTON P.M., MEIER T., KING P. 1991. Segmentation, neurogenesis and formation of early axonal pathways in the centipede, *Ethmostigmus rubripes* (Brandt). – Wilhelm Roux's Archives of Developmental Biology **199**: 349–363.

WHITINGTON P.M., LEACH D., SANDEMAN R. 1993. Evolutionary change in neural development within the arthropods: axonogenesis in the embryos of two crustaceans. – Development **118**: 449–461.

WHITINGTON P.M., BACON J.P. 1998. The organization and development of the arthropod ventral nerve cord: insights into arthropod relationships. Pp. 349–367 in: FORTEY R.A., THOMAS R.H. (eds), Arthropod Relationships. The Systematics Association Special Volume Series. – Springer, Netherlands.

WOLFF G.H., THOEN H.H., MARSHALL J., SAYRE M.E., STRAUSFELD N.J. 2017. An insect-like mushroom body in a crustacean brain. – eLIFE **6**:e29889.